energies

MDPI

Review

Machine Learning Applications in CO_2 Geological Sequestration: A Review of Pre-Injection Evaluation, Injection Optimization, and Post-Injection Monitoring

Watheq J. Al-Mudhafar [1,*], Ahmed Alsubaih [2] and Kamy Sepehrnoori [2]

[1] Basrah Oil Company, Basrah 61001, Iraq
[2] Hildebrand Department of Petroleum and Geosystems Engineering, The University of Texas at Austin, Austin, TX 78712, USA; aaa8649@my.utexas.edu (A.A.); kamys@mail.utexas.edu (K.S.)
* Correspondence: watheq.almudhafar@utexas.edu

Abstract

Rising atmospheric CO_2 levels pose a critical challenge to achieving global sustainability targets. Geological carbon sequestration (GCS) offers a long-term solution for reducing greenhouse gas emissions, but its large-scale deployment faces limitations in cost, uncertainty, and operational risk. Recent advances in machine learning (ML) present transformative opportunities to enhance every stage of the carbon capture and storage (CCS) lifecycle, from pre-injection evaluation to post-injection monitoring. This review systematically examines ML integration in CCS applications, emphasizing roles in geological characterization, injection optimization, plume prediction, and leakage detection. It provides a structured overview of ML methodologies including Random Forest, Support Vector Regression, and XGBoost, along with emerging deep learning models used for anomaly detection and uncertainty quantification. Experimental insights, monitoring techniques, and real-time data applications are summarized to illustrate ML's capability in accelerating simulations, reducing costs, and increasing safety assurance. Furthermore, real-world case studies such as Sleipner (Norway), Illinois Basin–Decatur (USA), Boundary Dam (Canada), Gorgon (Australia), and Quest (Canada) demonstrate how ML has enhanced performance, predictive accuracy, and storage reliability in field-scale CCS projects. The review concludes by identifying existing challenges, data scarcity, interpretability, and regulatory integration, and proposes a unified ML framework for scalable, autonomous, and secure CO_2 storage. Overall, this study provides a comprehensive roadmap for leveraging artificial intelligence to achieve reliable, cost-effective, and sustainable carbon management solutions aligned with global net-zero objectives.

Keywords: carbon capture and storage; machine learning; geological sequestration; injection optimization; anomaly detection; post-injection monitoring

Academic Editors: Zheyu Liu, Bo Liao, Maojie Chai, Zuhao Kou and Zhe Sun

Received: 17 May 2026
Revised: 19 June 2026
Accepted: 26 June 2026
Published: 30 June 2026

1. Introduction

Rising atmospheric concentrations of carbon dioxide (CO_2) pose one of the most critical challenges to achieving global environmental sustainability. As a major greenhouse gas, CO_2 contributes nearly 30% of total emissions and remains a principal driver of global warming. The primary sources of these emissions are the combustion of petroleum products and coal, which also exacerbate environmental degradation through acid rain formation. Despite decades of international awareness campaigns and climate conferences, such as the Munich Climate Conference, efforts to curb emissions have yielded limited progress.

Since renewable and low-carbon energy sources alone cannot fulfill the world's net-zero emission targets, alternative strategies such as geological carbon sequestration (GCS) have become increasingly vital. Meanwhile, recent advances in machine learning (ML) present powerful tools to enhance the efficiency, reliability, and predictive capability of GCS systems. Accordingly, this introduction outlines (1) the environmental challenge and the rationale for adopting GCS, (2) the potential role and benefits of ML in CO_2 sequestration, and (3) the motivation, challenges, and objectives of this study. The overall framework of the research, illustrating how ML methods integrate across the carbon capture and storage (CCS) lifecycle from pre-injection evaluation to post-injection monitoring, is depicted in Figure 1.

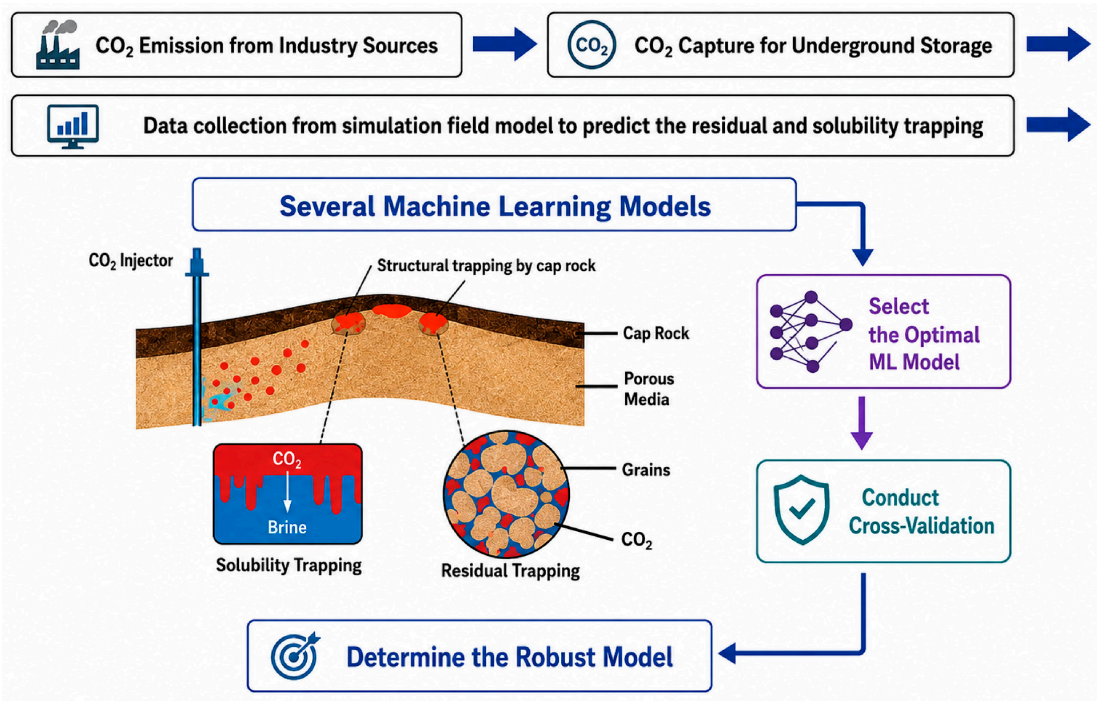

Figure 1. Study framework illustrating the integration of machine learning across the carbon capture and storage (CCS) lifecycle.

To establish a clear framework for understanding how machine learning (ML) integrates across the various stages of the carbon capture and storage (CCS) lifecycle, this review is structured into six major sections. Section 2 provides a detailed examination of ML applications in pre-injection evaluation and site selection, emphasizing geological characterization, storage capacity estimation, and risk assessment techniques. Section 3 addresses injection and storage optimization, with particular focus on surrogate modeling, reinforcement learning, and hybrid methodologies designed to enhance injection strategies and reservoir management. Section 4 investigates post-injection monitoring and leakage detection, highlighting ML-driven anomaly detection frameworks, environmental risk assessments, and subsurface data interpretation. Section 5 reviews real-world case studies, including the Sleipner, Illinois Basin–Decatur, and Boundary Dam projects, to demonstrate the practical benefits, challenges, and outcomes of ML applications in CCS operations. Finally, Section 6 presents the overall conclusions, synthesizing the main insights discussed throughout the paper and identifying future research priorities essential for achieving scalable, autonomous, and cost-effective CCS solutions. This structured organization offers a holistic view of the rapidly advancing role of ML in enhancing the efficiency, safety, and sustainability of carbon sequestration projects.

1.1. The Environmental Challenge and the Role of Geological Carbon Sequestration

The continued dependence on fossil fuels, driven by industrial growth and global economic competition, has resulted in a persistent increase in CO_2 emissions. These emissions are the principal drivers of climate change and contribute to transboundary environmental challenges such as ocean acidification and air pollution. Although numerous international initiatives have sought to curb CO_2 emissions, their progress has been constrained by economic, political, and logistical barriers.

In parallel with the global transition toward cleaner energy sources, geological carbon sequestration (GCS) has emerged as a promising strategy to mitigate atmospheric CO_2 accumulation. GCS entails the long-term storage of carbon dioxide within deep subsurface geological formations, including saline aquifers, depleted oil and gas reservoirs, and unmineable coal seams.

The injected CO_2 can be securely retained through several trapping mechanisms, as illustrated in Figure 2:

1. Structural trapping, in which CO_2 is physically confined beneath impermeable caprocks;
2. Residual trapping, where CO_2 becomes immobilized within pore spaces by capillary forces;
3. Solubility trapping, through which CO_2 dissolves into formation water;
4. Mineral trapping, where CO_2 reacts with host rock minerals to form stable carbonate compounds [1].

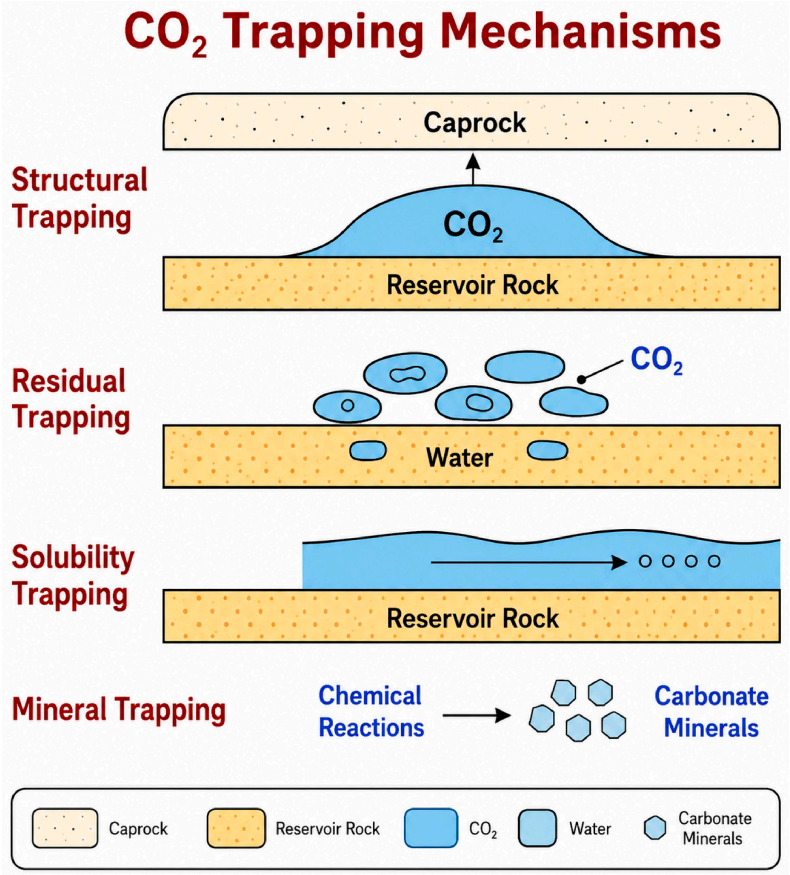

Figure 2. Trapping mechanisms of carbon dioxide (CO_2).

Certain storage mechanisms necessitate comprehensive site characterization, particularly regarding porosity, permeability, fracture pressure, and caprock integrity, to ensure adequate storage capacity and to prevent potential CO_2 leakage [2–4].

1.2. The Role of Machine Learning in Carbon Storage: Capabilities and Challenges

Artificial intelligence (AI) has opened new avenues for optimizing carbon dioxide sequestration, with machine learning (ML) emerging as one of the most relevant and transformative domains. ML algorithms enable the energy industry to efficiently process large datasets, uncover hidden patterns, and make high-speed predictions. In the context of geological carbon sequestration (GCS), ML offers several advantages over conventional reservoir simulation tools, which often demand extensive subsurface data and significant computational resources. Based on the learning approach employed, ML methods can be broadly categorized into two main types:

1. Supervised learning, which relies on labeled input–output datasets to predict target variables such as CO_2 trapping efficiency;
2. Unsupervised learning, which identifies hidden structures or anomalies within data that may indicate potential leakage pathways or geological instabilities [5–7].

Machine learning has proven particularly effective in real-time monitoring systems, where it can detect irregular pressure signals, fluid flow anomalies, and induced seismicity by analyzing seismic and geophysical sensor data [7]. ML techniques can also optimize injection strategies by recommending optimal pressure levels and injection rates, thereby minimizing fracture risks while improving overall process efficiency [8].

Recent studies have demonstrated the predictive capabilities of ML in modeling CO_2 behavior. For instance, Menad et al. [9] employed artificial neural networks (ANNs) to predict CO_2 solubility in brine aquifers with high accuracy. Similarly, Mahdaviara et al. [10], Al-Mudhafar [11], Jeong et al. [12], and Ganesh and Mishra [13] utilized various ML approaches, such as multivariate regression, support vector regression (SVR), and adaptive splines, to forecast CO_2 injection performance and storage efficiency. Zhang et al. [14] applied the Extreme Gradient Boosting (XGBoost) algorithm to estimate the optimal injection depth in saline formations. Recent large-scale comparative studies have further validated XGBoost's superiority for CCS applications. Vo Thanh and Lee [15] conducted a comprehensive study using 1509 field-scale simulation samples from the global literature. They compared XGBoost, Random Forest (RF), and Support Vector Regression (SVR). Their results demonstrated that XGBoost consistently outperformed both RF and SVR, achieving an extremely low root mean square error (RMSE = 0.0041) and a high correlation factor (R^2 = 0.9993) for both residual and solubility trapping efficiency. Critically, this study emphasized that using global field data rather than synthetic reservoir models significantly enhances model generalizability and practical applicability, a key consideration for real-world CCS projects. Figure 3 categorizes the primary ML algorithm families commonly used in CO_2 modeling and prediction:

1. Linear models;
2. Decision tree methods (e.g., Random Forest);
3. Neural network architectures (e.g., ANN);
4. Ensemble methods (e.g., XGBoost, which integrates multiple weak learners to achieve strong predictive performance).

Beyond predicting CO_2 trapping efficiency, machine learning has been successfully applied to optimize cement formulations for CCS wells. Alsubaih et al. [16] developed a knowledge-guided ML framework using ensemble learning models (Random Forest, Gradient Boosting, AdaBoost, XGBoost, and CatBoost) to predict compressive strength and thermal stability of cement formulations for geothermal and CO_2 storage wells. Using a dataset of over 360 laboratory cement tests, CatBoostRegressor achieved superior predictive performance with a test R^2 of 0.9873 and RMSE of 9.92 °C. The optimized formulations achieved predicted compressive strengths exceeding 7000 psi and temperature suitability

above 300 °C, demonstrating that ML can accelerate the design of thermally resilient cement systems for extreme subsurface environments.

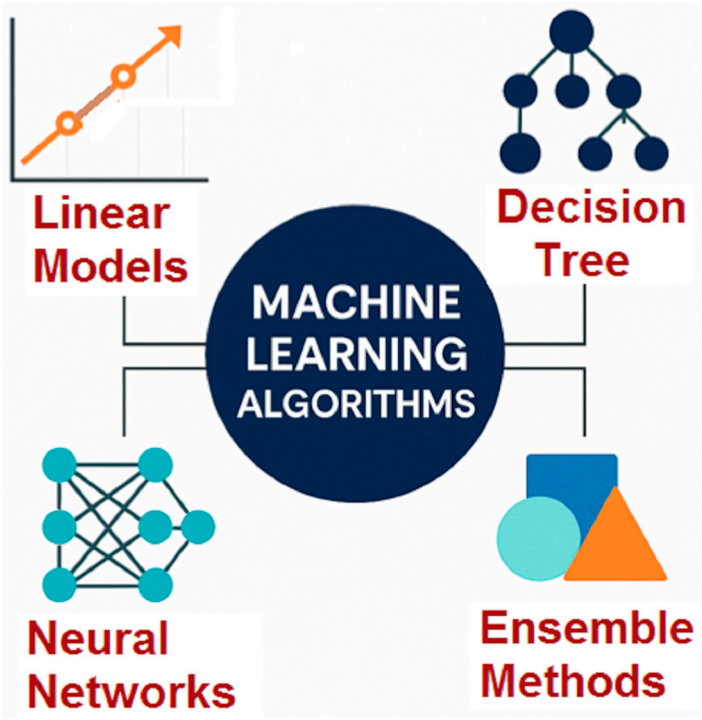

Figure 3. Machine learning algorithms in carbon sequestration.

Despite these advancements, several challenges have limited the widespread application of ML in GCS. Many models are trained on data derived from homogeneous synthetic reservoirs, making them less applicable to the complexity of real-world geological systems. Additionally, subsurface datasets are often heterogeneous, expensive to obtain, and limited in quantity, reducing model generalizability.

Although deep learning models exhibit strong predictive capabilities, they are often regarded as "black boxes" raising concerns about their interpretability and trustworthiness in safety-critical applications such as CO_2 storage [17]. Figure 4 provides a comparative radar chart of six ML algorithm families across five critical dimensions: predictive accuracy, interpretability, data efficiency, computational cost, and regulatory acceptance. Furthermore, large-scale implementation of ML solutions faces infrastructural, computational, and regulatory challenges, including high computational costs, integration difficulties with legacy CCS systems, and inconsistent policy frameworks across regions [12,13].

1.3. Research Motivation, Objectives, and Study Framework

Conventional compositional reservoir simulations can effectively model fluid behavior and CO_2 trapping mechanisms, particularly residual and solubility trapping, as demonstrated in several previous studies [9,12–14,18–20]. However, the computational time required for field-scale models, which often consist of millions of grid blocks, is prohibitively high, rendering their implementation both technologically and economically challenging. Producing a reliable forecast of CO_2 trapping efficiency can take several days or even weeks. These challenges underscore the need for efficient surrogate modeling techniques capable of drastically reducing computational cost and simulation time, an area where machine learning (ML) has demonstrated significant potential [21–25].

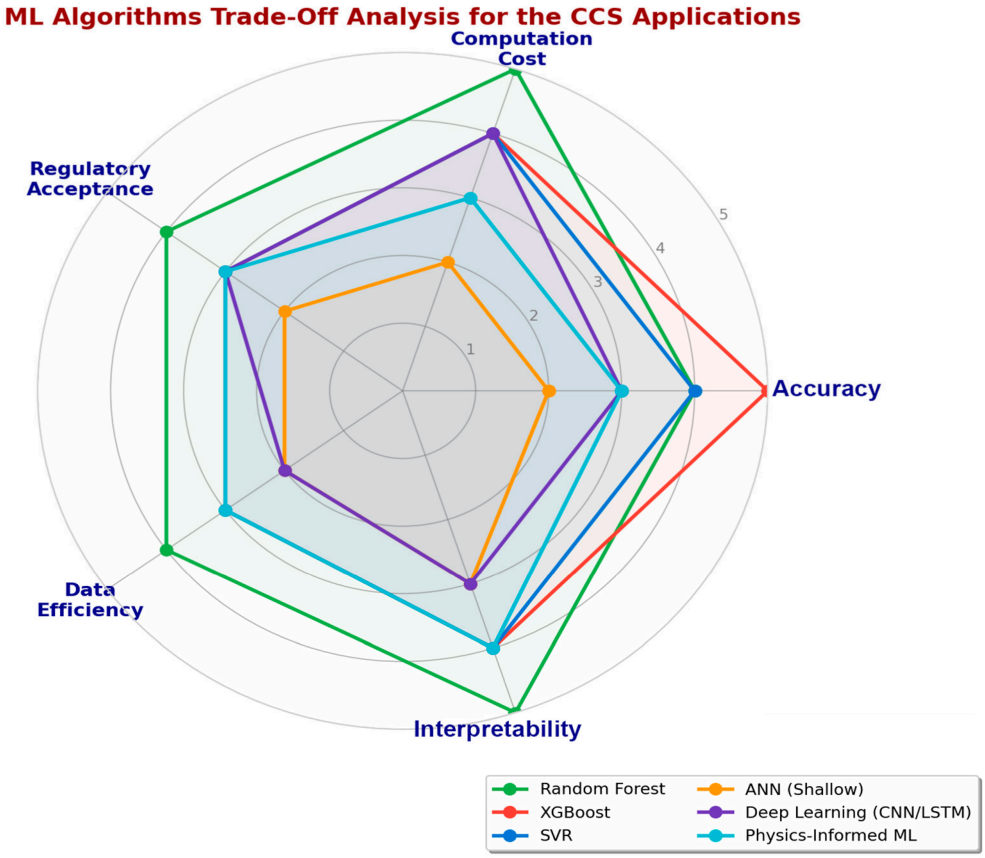

Figure 4. Comparative trade-off analysis of machine learning algorithms for CCS applications. Radar chart comparing six algorithm families across five dimensions: predictive accuracy (R^2 from CCS literature), interpretability (model transparency), data efficiency (performance with limited training data), computational cost (training time and resources), and regulatory acceptance (suitability for safety-critical decisions). XGBoost and deep learning methods achieve the highest accuracy ($R^2 > 0.97$) but suffer from low interpretability. Random Forest offers the best balance ($R^2 \approx 0.91$ with high interpretability), making it suitable for regulatory-sensitive applications such as site selection and risk assessment.

Despite their promise, most existing ML models have been developed using synthetic or oversimplified datasets, which limits their applicability to the complex geological realities of actual storage sites. To address this gap, the present study emphasizes training ML models on real-world field data compiled from the literature and global CCS case studies. In this research, three widely adopted ML algorithms were examined:

1. Random Forest (RF), recognized for its interpretability and robustness when handling large, noisy datasets [9,14,18–20];
2. Support Vector Regression (SVR), known for its capability to model complex nonlinear regression relationships [12,13];
3. Extreme Gradient Boosting (XGBoost), a high-performance boosting technique that delivers superior accuracy and strong resistance to overfitting [14,20–23].

The complete workflow adopted in this study is illustrated in Figure 1, which outlines the methodology in sequential stages: data acquisition and preprocessing, ML model selection, training and prediction, and performance evaluation of CO_2 injection outcomes. This framework integrates geological, physical, and algorithmic components to enable fast and accurate estimation of sequestration efficiency.

The main objectives of this research are as follows:

1. To develop a comprehensive synthesis of ML applications across the CCS lifecycle, encompassing site selection, injection optimization, and post-injection monitoring;
2. To build an inventory and classification of CCS datasets used in ML studies, identifying geological, petrophysical, and dynamic features relevant for model training;
3. To compare and evaluate ML algorithms such as RF, SVR, and XGBoost in predicting CO_2 storage potential under varying subsurface conditions;
4. To assess the effectiveness of ML tools in reducing simulation time, identifying real-time anomalies, and improving CO_2 plume management;
5. To examine global CCS case studies demonstrating ML deployment, extracting practical insights and lessons for future projects;
6. To evaluate the long-term sustainability of CO_2 storage, emphasizing ML's role in uncertainty quantification, risk assessment, and decision support frameworks.

This research ultimately aligns with the global transition toward carbon-neutral energy systems. According to the Global CCS Institute, as of 2025, 79 commercial CCS plants are in operation worldwide, with more than 628 projects under development, an increase of over 60% within two years. Collectively, these facilities capture more than 50 million tonnes of CO_2 annually; however, achieving global net-zero targets will require increasing this capacity to approximately 1.3 billion tonnes per year by 2050. Machine learning has the potential to transform this trajectory by enabling data-driven site evaluation, reducing operational costs, and improving system integrity through real-time monitoring and predictive analytics. Recent studies have shown that ML systems can reduce CO_2 capture costs by 20–30%, improve the accuracy of leak detection, and accelerate decision-making across integrated subsurface, seismic, and operational datasets [24–32].

Despite the growing body of literature on ML applications in CCS, significant gaps remain. As shown through a systematic comparison with five previous reviews (Section 1.4; Table 1), existing reviews exhibit fragmented scope, limited critical analysis of ML trade-offs, insufficient field-scale validation, and a lack of unified frameworks that connect algorithm selection to operational decision-making and regulatory requirements. Furthermore, the reliance on synthetic datasets in many ML studies, while a common limitation, has not been systematically addressed in the review literature through a framework that guides practitioners in selecting appropriate ML methods based on data availability and application context. This review addresses these gaps by providing a comprehensive, lifecycle-oriented synthesis that integrates critical algorithm evaluation, field-scale case studies, and a practical decision-support framework for CCS practitioners.

Table 1. Comparison of this review with previous reviews on ML in CCS.

Review	Scope	ML Methods Covered	Case Studies	Unique Contribution
Gupta and Li (2022) [33]	General ML for CO_2 sequestration, storage, transport, and utilization	Overview of RF, ANN, SVM, XGBoost	Limited	Broad perspective on ML across entire CCUS value chain
Rehman and Lal (2023) [34]	ML in CO_2 sequestration	RF, ANN, SVM, deep learning	Limited	Focus on flow assurance and production
Vo Thanh and Lee (2022) [15]	ML for CO_2 storage performance prediction	XGBoost, RF, SVR	Limited (field validation)	Quantitative comparison of ML algorithms using global field data
Alsubaih et al. (2025) [35]	Well integrity and digital twins	Ensemble learning (CatBoost, XGBoost)	Limited	Focus on cement integrity, digital twins
Yan et al. (2022) [36]	Deep learning for plume prediction	FNO, CNN, LSTM	Limited	Deep learning surrogates for multiphase flow

Table 1. *Cont.*

Review	Scope	ML Methods Covered	Case Studies	Unique Contribution
This Review	Full CCS lifecycle (pre-injection → injection → post-injection)	RF, SVR, XGBoost, GPR, ANN, CNN, LSTM, FNO, ensemble methods	7 field-scale projects (Sleipner, IBDP, Boundary Dam, Gorgon, Quest, Teapot Dome, orphan wells)	Unified ML framework; critical algorithm trade-off analysis; regulatory acceptance; digital twin integration; legacy well risk assessment

1.4. Comparison with Previous Reviews

To establish the novelty and contribution of this review, it is essential to position it relative to existing comprehensive reviews on machine learning in carbon capture and storage. Table 1 provides a structured comparison of this work with five representative review papers, evaluated across four dimensions: scope (CCS lifecycle stages covered), ML methods discussed, case study integration, and unique contributions.

As summarized in Table 1, previous reviews exhibit several limitations that this work addresses:

1. Fragmented scope: Most existing reviews focus on isolated CCS stages, either pre-injection characterization [35], injection optimization [34], or post-injection monitoring [37], without providing an integrated lifecycle perspective. This review systematically examines ML applications across all three stages, emphasizing their interconnections and cumulative value.
2. Limited critical analysis of ML trade-offs: While previous reviews describe ML algorithms and their reported accuracies, few critically examine the trade-offs between accuracy, interpretability, data efficiency, computational cost, and regulatory acceptance, a dimension essential for practical deployment in safety-critical CCS applications. This review provides a structured comparative analysis (Figure 4) of these trade-offs across six algorithm families.
3. Insufficient field-scale validation: Most reviews rely heavily on synthetic or laboratory-scale studies, with limited integration of real-world CCS project experiences. This review synthesizes lessons from seven field-scale projects (Sleipner, Illinois Basin-Decatur, Boundary Dam, Gorgon, Quest, Teapot Dome, and orphan well risk assessment), providing practical insights for operators and regulators.
4. Lack of unified framework: No previous review proposes a unified ML framework that connects algorithm selection to specific CCS tasks, data availability, and regulatory requirements. This review addresses this gap by proposing a decision-support framework that guides practitioners in selecting appropriate ML methods based on their specific application context.
5. Limited coverage of emerging topics: Digital twin technology, AI-driven well integrity monitoring, and legacy well risk assessment, critical for large-scale CCS deployment, are underrepresented in previous reviews. This review dedicates dedicated subsections to these emerging applications.

Thus, while previous reviews provide valuable contributions to specific aspects of ML in CCS, this review offers a comprehensive, critically analytical, and practice-oriented synthesis that bridges the gap between ML research and CCS operational deployment.

2. Pre-Injection Analysis

Geological carbon sequestration (GCS) requires rigorous pre-injection analysis to ensure long-term safety, operational efficiency, and regulatory compliance. This section

provides a detailed overview of the three key components of pre-injection assessment: reservoir characterization, capacity estimation, and storage site selection. Recent advances in machine learning (ML) and geoscientific techniques are integrated into these domains, offering a comprehensive review of current methodologies and research developments.

2.1. Reservoir Characterization

Accurate reservoir characterization is fundamental to identifying suitable geological formations for CO_2 storage. It involves assessing rock properties such as porosity, permeability, heterogeneity, and caprock integrity, which collectively determine the storage capacity and containment effectiveness of a formation [21]. In recent years, artificial intelligence (AI) and ML have become increasingly important tools for managing large, complex datasets and enhancing predictive modeling of subsurface behavior [22–24].

2.1.1. Geomechanical Properties and Their Role in Storage Integrity

The success of CO_2 sequestration projects depends critically on understanding key geomechanical parameters that govern rock behavior under stress. Among these, Unconfined Compressive Strength (UCS) represents the maximum axial stress a rock sample can withstand under zero confining pressure before failure. UCS is fundamental to determining safe injection pressures, as exceeding the UCS of reservoir or caprock formations can induce fracturing, creating unintended leakage pathways [38]. Low UCS values particularly increase the probability of fault reactivation under pressure, leading to microseismic events or reservoir damage [39].

Young's Modulus (E), the ratio of normal stress to strain within the proportional limit, characterizes rock stiffness. Rocks with higher Young's modulus exhibit greater resistance to deformation under stress, which is advantageous for maintaining caprock integrity during pressure cycling associated with CO_2 injection. Conversely, low Young's modulus values may require additional preventive measures such as casing optimization or reduced injection rates to ensure long-term wellbore stability [40,41].

Poisson's Ratio (ν), which describes the ratio of lateral to axial strain under compression, plays a critical role in fracture pressure gradient prediction. Poisson's ratio typically increases with depth, ranging from 0.2 to 0.25 in shallow formations to approaching 0.5 in deeply compacted rocks. This variability directly affects horizontal stress magnitudes, higher Poisson's ratios correlate with greater horizontal stress, influencing fracture initiation pressures and fault reactivation potential [42,43]. Accurate knowledge of Poisson's ratio is therefore essential for determining appropriate injection pressures and mud weight windows during drilling operations [44].

Recent advances in understanding wellbore cement degradation under CO_2 exposure have revealed the critical importance of coupled thermoporoelastic effects. Alsubaih et al. [35] developed a fully coupled 3D thermoporoelastic model to simulate stress distribution within wellbore systems, integrating thermal and mechanical properties with pressure and temperature boundary conditions to solve for hoop, radial, and axial stresses. Their sensitivity analysis identified Young's modulus and thermal expansion coefficient of sandstone, casing, and cement as the most influential factors affecting stress components, with variations in these properties leading to changes in radial stress exceeding 30%. The study also incorporated chemical degradation effects using PHREEQC, simulating dissolution and precipitation reactions that influence porosity, permeability, and mechanical properties. This comprehensive thermo-hydro-chemo-mechanical (THCM) analysis revealed that porosity and permeability dynamically evolve due to chemical reactions, significantly influencing stress distribution and failure risks in the cement sheath.

The integration of chemical degradation effects is particularly critical for CCS applications. Alsubaih et al. [35] demonstrated that self-healing cement formulations incorporating Barite, Pozzolan, and Chalcedony can reduce porosity by 3–4% within 7–14 days through the formation of calcium silicate hydrate (C-S-H) gels, enhancing crack sealing and mechanical resilience. Compared to conventional cement (which shows progressive porosity increase exceeding 17% over time), these self-healing formulations maintained long-term structural integrity under CO_2-rich conditions, with saturation index trends confirming the stability of key mineral phases (ECSH2 and Calcite).

Machine learning has emerged as a powerful tool for predicting these geomechanical properties. Gowida et al. [45] demonstrated real-time UCS prediction while drilling using artificial intelligence tools, achieving significant cost and time savings compared to traditional laboratory testing. Similarly, Siddig et al. [46] developed ANN and ANFIS models for real-time Poisson's ratio prediction from drilling parameters, achieving correlation coefficients between 0.98 and 0.99 with errors of only 1–2%. These advances enable more dynamic and responsive reservoir management during CCS operations.

2.1.2. Modern Scientific Methods

Advanced geophysical and geostatistical techniques have revolutionized the accuracy of reservoir characterization. Three-dimensional seismic imaging and other high-resolution geophysical methods enable detailed mapping of structural traps and subsurface heterogeneities [25]. Geostatistical modeling and petrophysical analyses, based on well log and core data, provide valuable insights into pore structures and flow dynamics within the reservoir [26].

ML algorithms, such as support vector regression (SVR), artificial neural networks (ANNs), and ensemble learning models, have proven particularly effective for interpolating missing data and predicting parameters that are otherwise difficult to measure directly [27–29]. In reservoir monitoring, convolutional neural networks (CNNs) have been successfully applied to 4D seismic datasets for early detection of CO_2 migration pathways and potential leakage zones [30]. Furthermore, predictive ML models developed using real-time operational data can simulate various injection scenarios and recommend optimized injection strategies [31].

2.1.3. Importance and Benefits

Robust reservoir characterization is essential for effective site selection, maximized storage capacity, and minimized risks of leakage or induced seismicity. Integrating AI into geological evaluations enables significant automation and efficiency, reducing both time and cost while improving accuracy. This approach not only enhances the reliability of CO_2 storage projects but also provides considerable economic and environmental benefits [32].

2.1.4. Challenges and Risks

Despite recent advancements, several challenges persist in achieving comprehensive reservoir characterization. These include limited availability of high-quality geological data, complex subsurface heterogeneities, and the high cost associated with data acquisition and analysis [47]. Insufficient characterization can lead to underestimation of crucial risks, such as caprock failure or lateral CO_2 migration, potentially compromising storage integrity [48].

2.1.5. Equipment and Tools

Reservoir characterization for CO_2 sequestration primarily involves the use of seismic imaging tools to generate three-dimensional maps of subsurface formations and identify structural features critical for CO_2 containment. Core-sample analysis is also essential for

quantifying petrophysical properties such as porosity and permeability, which are vital for static reservoir modeling.

Various reservoir flow simulation tools are widely used to model fluid flow mechanisms, CO_2 plume migration, and trapping behavior under different injection scenarios. These tools are now increasingly enhanced by AI-integrated platforms, which automate data processing, improve simulation accuracy, and enable real-time detection of anomalies in pressure and temperature data. The fusion of ML with conventional reservoir engineering tools has made geological and geophysical analyses more efficient and reliable, significantly accelerating site evaluation and decision-making [49–51].

Machine learning and conventional modeling tools together underpin the major tasks in pre-injection analysis, reservoir characterization, capacity estimation, and site selection, while addressing key challenges such as data scarcity, uncertainty, and high operational costs. Table 2 provides a comparative overview of the principal methods, their advantages, and the technological enablers used in each domain, highlighting the synergy between traditional approaches and emerging AI-driven techniques.

Table 2. Comparison of Pre-Injection Analysis Techniques.

Reference	Aspect	Reservoir Characterization	Capacity Estimation	Site Selection
Baz et al. [2]; Soltanian et al. [3]	Key Methods	3D seismic analysis, AI-driven modeling, petrophysical analysis	Computer modeling, geological volume analysis, pilot injection tests	Multicriteria algorithms, geological surveys
Sohal et al. [4]; Singh et al. [5]	Challenges	Data scarcity, high costs, geological uncertainty	Geological uncertainty, high costs of field experiments	Accessibility, public perception, land use conflicts
Dejam and Hassanzadeh [6]; Szulczewski et al. [7]	Benefits	Enhanced precision, safety, and efficiency	Accurate storage capacity estimation, risk management	Optimal site selection, reduced exploration risk
Nghiem et al. [8]; Vo Thanh et al. [17]	Tools/Technologies	Seismic imaging, geostatistical modeling, AI algorithms	ECLIPSE, CMG GEM, pilot injection tests	GIS, machine learning algorithms

2.2. Capacity Estimation

The capacity estimation of a geological formation is a critical component of feasibility studies and a prerequisite for regulatory approval of carbon storage projects. The accuracy of such estimates depends heavily on the underlying geological parameters and the type of computational modeling employed.

2.2.1. Simulation-Based Estimation

Simulation models replicate subsurface dynamics to predict CO_2 plume migration, solubility, and trapping mechanisms. Traditional reservoir simulators such as ECLIPSE and CMG-GEM have long been used to simulate complex fluid interactions under reservoir conditions, incorporating temperature, pressure, and mineralization effects [1,52,53]. However, these simulations are computationally intensive. With recent advances, ML-based surrogate models have emerged as efficient alternatives, offering comparable accuracy while significantly reducing computational time and cost [33,34,54].

Several recent studies have systematically compared multiple ML algorithms to identify the most accurate and reliable models for predicting CO_2 trapping efficiency. Safaei-

Farouji et al. [55] evaluated four ML models, Adaptive Neuro-Fuzzy Inference System (ANFIS), Extra Tree (ET), Random Forest (RF), and Radial Basis Function (RBF), using 1868 field simulation data points. Their results showed that RF achieved the highest accuracy, with R^2 values of 0.995 and 0.965 for residual and solubility trapping indices, respectively. The ranking of model performance was RF > ANFIS > RBF > ET. Sensitivity analysis using the relevancy factor revealed that depth and post-injection time were the most influential factors for residual and solubility trapping, respectively.

Vo Thanh and Lee [15] applied Gaussian Process Regression (GPR), SVM, and RF to predict CO_2 trapping performance in deep saline aquifers. The GPR model demonstrated superior performance with R^2 = 0.992 and RMSE = 0.00491, outperforming both SVM and RF. The study validated the GPR model using field data from the Cuu Long Basin offshore Vietnam, achieving R^2 values of 0.999 and 0.9935 for solubility and residual trapping indices, respectively. This field validation confirms the practical applicability of ML models for real-world CCS projects.

More recently, Abdulkhaleq et al. [56] applied RBF-NN proxy modeling to optimize CO_2 sequestration in the Tensleep formation at Teapot Dome, Wyoming. Using Latin Hypercube Sampling (LHS) to generate 100 simulation runs, the RBF-NN proxy model achieved R^2 values of 0.962, 0.847, and 0.849 for total trapped CO_2, total trapping index, and leakage index, respectively. The optimization enhanced total trapping efficiency from 75% to 83% with only a minor increase in leakage index (0.64% to 1.3%), demonstrating the effectiveness of proxy-based optimization for CCS applications. Abdulwahab et al. [57] developed an NN-RBF surrogate model achieving R^2 = 0.982 for emulating full-physics simulation responses, enabling rapid optimization of CO_2 injection and DWS operations. Al-Mudhafar and Abdulwahid [58] further demonstrated that RBF-ANN can achieve R^2 = 1.000 for trapping efficiency prediction in fully water-saturated reservoirs, significantly outperforming polynomial regression (R^2 = 0.586–0.687). These findings confirm that RBF-based neural networks provide reliable, computationally efficient alternatives to full-physics simulation for capacity estimation and optimization.

Figure 5 compares the predictive performance (R^2 values) of four widely used ML models for CO_2-related predictions, with ranges compiled from multiple studies including Menad et al. [9], Zhang et al. [14], and Mahdaviara et al. [16]. Random Forest (RF) achieves R^2 values of 0.90–0.91, Support Vector Regression (SVR) achieves 0.92–0.93, Artificial Neural Networks (ANN) achieve 0.94–0.95, and XGBoost achieves the highest performance at 0.97–0.98. Notably, some studies have reported even higher performance for XGBoost (e.g., R^2 = 0.9993, Vo Thanh and Lee [15]), reflecting the influence of dataset size, quality, and application context on reported metrics. These performance metrics inform model selection decisions for specific CCS applications.

2.2.2. Geological Volume and Pore Space Analysis

Geological evaluations typically involve calculating effective pore volume, taking into account formation thickness, porosity, and fluid saturation. These analyses help estimate the total amount of CO_2 that can be securely stored in both free and residual forms, thereby quantifying the effective storage capacity of a given reservoir [59,60].

2.2.3. Pilot Injection Tests

Pilot-scale injection tests are conducted to inject limited volumes of CO_2 and observe pressure responses, fluid migration, and potential leakage pathways. These experiments are essential for calibrating simulation models and identifying operational risks early, thereby enabling the mitigation of potential failures before full-scale deployment [61].

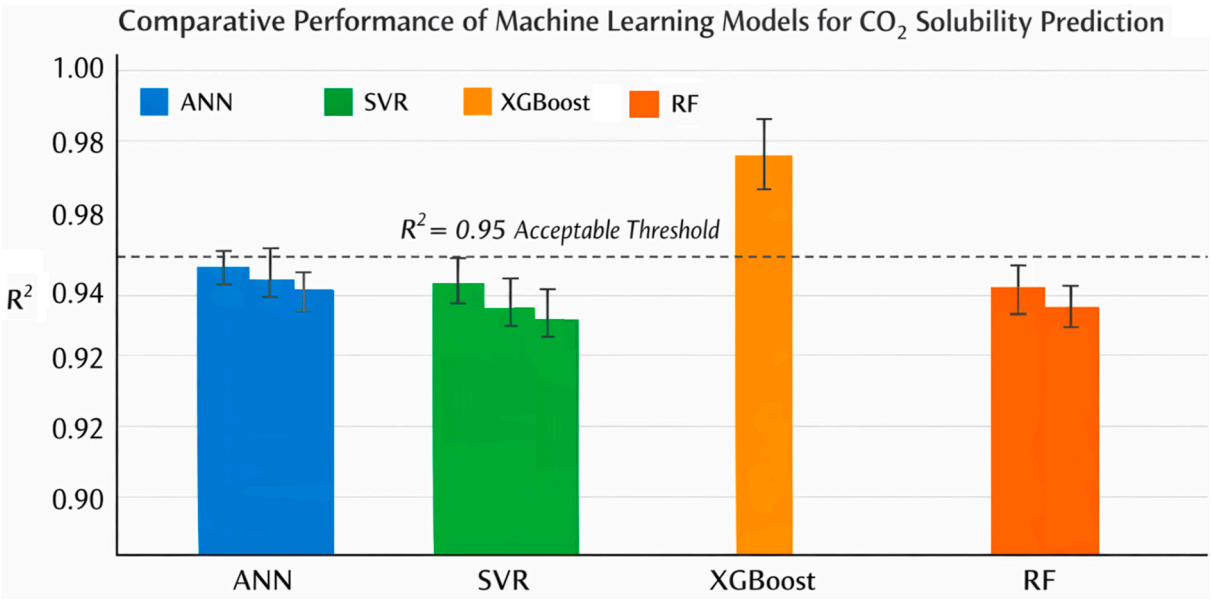

Figure 5. Comparative performance of machine learning models for CO_2-related predictions in CCS applications. R^2 values are compiled from multiple studies including Menad et al. [9], Zhang et al. [14], and Mahdaviara et al. [10]. Individual studies may report higher or lower values depending on dataset characteristics; for example, Vo Thanh et al. (2022) [15] achieved R^2 = 0.9993 for XGBoost on a global field dataset. The dashed line at R^2 = 0.95 represents the commonly accepted threshold for "good" predictive performance in geoscience applications. XGBoost consistently achieves the highest accuracy across studies, while Random Forest offers competitive performance with superior interpretability. These trade-offs inform model selection decisions based on specific CCS application requirements (e.g., regulatory acceptance may favor interpretable RF models, while high-accuracy predictions may favor XGBoost).

2.2.4. Challenges and Considerations

Accurate capacity estimation remains challenged by reservoir heterogeneity, complex flow behavior, and geochemical interactions within the storage formation. Additional obstacles include the high cost of field testing, limited data availability, and restricted access to suitable sites [62]. However, emerging ML-assisted capacity estimation methods, particularly those that integrate real-time monitoring and data assimilation, have shown great promise in reducing uncertainty and improving predictive accuracy [63].

2.3. Storage Site Selection

Selecting an appropriate storage site is one of the most critical decisions in geological carbon sequestration (GCS), as it directly affects the project's viability, safety, and long-term success. A thorough evaluation must incorporate geological, technical, environmental, and socio-economic criteria to ensure that the site can securely contain large volumes of CO_2 for decades or even centuries, with minimal leakage risk. Potential storage sites include depleted oil and gas fields, deep saline aquifers, and unmineable coal seams, each offering distinct advantages and limitations. Depleted reservoirs are often preferred due to their proven geological seals and existing infrastructure, whereas saline aquifers provide vast storage capacity but require extensive geological characterization and carry higher exploration risk. Consequently, robust screening and ranking methods must be applied to balance these trade-offs and ensure optimal site selection.

Recent advancements in ML have transformed traditional site-selection workflows. As shown in Table 3, algorithms such as Random Forest (RF), Artificial Neural Networks (ANN), and Support Vector Regression (SVR) have been used to analyze large datasets encompassing geological, geophysical, and socio-economic variables. These models enhance

predictive accuracy and reduce uncertainty, significantly decreasing the time and cost associated with conventional exploration approaches. Despite limitations, such as sensitivity to input data quality and the need for frequent recalibration, ML-based frameworks have become powerful tools for conditional decision-making under uncertain or incomplete data environments.

Table 3. Comparison of Machine Learning Applications in CCS.

Reference	Application	ML Techniques Used	Key Benefits	Challenges
Wu et al. [64]; Damico et al. [65]	Site Selection	Random Forest, ANN, geostatistical modeling	Faster and more accurate site selection	Data scarcity, geological uncertainty
Chen et al. [19]; Jeong et al. [12]	Injection Optimization	SVR, XGBoost, neural networks	Optimized injection rates, reduced leakage risk	Requires real-time data, computational cost
Zhong et al. [66]; Zhang et al. [67]	Leakage Detection	Deep learning (CNN, LSTM), anomaly detection	Early detection of leaks, improved safety	High sensitivity to noise, false positives
Ganesh and Mishra [13]; Jeong et al. [12]	Long-Term Monitoring	ANN, Random Forest, simulation models	Continuous monitoring, predictive capabilities	Requires large datasets, model complexity

2.3.1. Technical Site Criteria

The technical suitability of a potential storage site is determined by its structural configuration, reservoir properties, and trapping mechanisms. Sites intended for long-term CO_2 storage should possess several favorable characteristics, including:

1. Tectonic stability, characterized by low seismic activity and the presence of a well-defined structural trap, such as an anticline or fault-bound reservoir [68].
2. Adequate depth (typically >800 m) to maintain CO_2 in a supercritical state, which increases its density and reduces mobility, thereby enhancing containment efficiency [69].
3. High porosity and permeability within the storage formation to ensure good injectivity and sufficient accommodation for large CO_2 volumes.
4. Caprock integrity, where the sealing layer must be impermeable and ductile rather than brittle or thin, to prevent upward CO_2 migration [70].
5. Hydrodynamic stability, ensuring predictable plume migration patterns that inform effective monitoring and long-term storage strategies [64].

These evaluations typically rely on seismic imaging, core sampling, well log interpretation, and geomechanical testing to validate structural and stratigraphic features. Once these properties are established, hydrogeologic modeling is used to simulate fluid flow paths and assess potential interactions between the injected CO_2 and native formation brines.

2.3.2. Socio-Economic Considerations

Beyond technical feasibility, socio-economic factors play a vital role in determining the practicality and long-term success of CO_2 storage projects. Key considerations include:

1. Infrastructure availability, particularly proximity to CO_2 emission sources (e.g., power plants or industrial facilities) and connectivity via existing pipeline networks. Sites located closer to emission hubs reduce transportation costs, improving overall project economics [65].

2. Land use and public perception, as onshore projects often face opposition related to environmental, safety, and property concerns, whereas offshore sites, though less socially constrained, typically involve higher operational costs and more complex regulatory requirements.
3. Legal and regulatory frameworks, which influence project permitting, long-term liability, and post-closure monitoring responsibilities.
4. Environmental and cultural protection zones, where areas of high biodiversity or heritage significance are generally excluded from development due to conservation laws or community resistance [71].

The availability and quality of geological data significantly affect both project cost and risk. High-resolution subsurface datasets, whether obtained from historical oil and gas exploration or new geophysical surveys, can greatly reduce uncertainty and attract investment by accelerating development timelines. Conversely, data-scarce regions often require substantial upfront investment in seismic acquisition and exploratory drilling [22,50].

3. Injection and Storage Optimization

Injection and storage optimization represent some of the most critical aspects of carbon capture and storage (CCS), ensuring efficient, secure, and long-term CO_2 injection into geological formations. This process combines computational modeling, real-time monitoring, and machine learning (ML) algorithms to maximize storage capacity while minimizing environmental and operational risks [72,73]. Three main optimization components are discussed in this section: injection rate control, plume prediction, and pressure monitoring.

3.1. Injection Rate Optimization

Optimizing the CO_2 injection rate is essential to achieving uniform distribution within the reservoir and avoiding excessive pressure buildup that could lead to leakage or fracturing. The optimization process depends on key reservoir parameters such as porosity, permeability, pressure, and temperature [74]. Conventional reservoir simulators are used to evaluate these parameters and determine the optimum injection conditions. More advanced optimization approaches employ shallow neural networks and genetic algorithms to jointly optimize injection rates and the placement of brine production wells [75]. These data-driven frameworks minimize trial-and-error and enable real-time adjustments to injection strategies. Continuous data acquisition from downhole sensors further supports optimization by providing live feedback for anomaly detection and operational decision-making [67,76].

Machine learning methods, particularly deep learning and artificial neural networks (ANNs), offer predictive insights and early warnings of undesirable reservoir behavior. By recognizing complex patterns in operational datasets, ML models can forecast plume migration behavior and reservoir response to different injection rates [36,77]. The Water-Alternating-Gas (WAG) injection strategy has been shown to enhance CO_2 trapping efficiency compared to continuous injection. Al-Khdheewai et al. [78] demonstrated that WAG injection improves residual and solubility trapping through enhanced macroscopic and microscopic sweep efficiencies. In heterogeneous fluvial sandstone reservoirs, WAG injection achieved approximately 25% higher total CO_2 trapping compared to continuous CO_2 injection, with residual trapping reaching 579,000 tons and solubility trapping reaching 296,000 tons over a 20-year injection period. This improvement is attributed to increased CO_2-water contact surface area and enhanced imbibition processes during cyclical injection.

Beyond WAG injection, the combination of Downhole Water Sink (DWS) technology with Huff and Puff (HnP) injection has demonstrated significant potential for enhancing CO_2 storage efficiency. Almansor et al. [79] evaluated DWS-HnP integration in the South Rumaila oil field, achieving a Total Trapping Index (TTI) of 0.99 and a Leakage Index (LI)

of 0.002, representing 99% trapping with only 0.2% leakage. The DWS system maintained reservoir pressure by producing water from the bottom layer, enhancing gas injectivity and enabling continuous injection over 19 years. This approach demonstrates that active pressure management through water extraction can significantly improve storage security while maintaining operational efficiency.

3.2. CO_2 Plume Prediction

Accurate plume prediction is essential for understanding the temporal and spatial evolution of CO_2 within the subsurface. It provides a safeguard against leakage risks and ensures regulatory compliance and long-term project viability [80].

3.2.1. Migration Dynamics

After injection, CO_2 tends to migrate upward through the reservoir along preferential pathways influenced by gravitational, viscous, and capillary forces. Geological heterogeneities, such as variations in porosity and permeability, strongly affect the shape and trajectory of the CO_2 plume. Faults and high-permeability zones accelerate plume migration, whereas low-permeability layers promote CO_2 trapping, contributing to storage stability.

3.2.2. Modeling and Simulation

To model plume dynamics, numerical simulations are used to solve the governing fluid flow equations in porous media, typically using finite difference or finite element methods. Integrating these simulations with geophysical and petrophysical datasets enhances the accuracy of plume predictions under real geological conditions. Recently, machine learning-assisted surrogate models have been developed to accelerate plume simulations, significantly reducing computational costs without compromising precision. Techniques such as graph neural networks (GNNs) and hybrid learning algorithms have achieved unprecedented accuracy in predicting CO_2 distribution within complex, faulted reservoirs [61,81].

A particularly promising development is the use of Fourier Neural Operator (FNO)-based deep learning workflows. Yan et al. [36] developed an FNO-based deep learning workflow to predict the temporal-spatial evolution of pressure and CO_2 plumes during injection and post-injection periods. Using a 3D heterogeneous saline aquifer model with 90 simulation runs (72 for training, 9 for validation, 9 for testing), the workflow achieved a speedup of 250 times compared to full physics reservoir simulation while maintaining high predictive fidelity. The study demonstrated two key design principles: (1) using separate deep learning models for injection and post-injection periods yields the most accurate pressure predictions, and (2) cumulative CO_2 injection volume is a critical feature for accurate saturation prediction, especially during the post-injection period when injection rates are zero.

Another promising development is the application of Physics-Informed Neural Networks (PINNs) to CCS problems. PINNs incorporate the governing partial differential equations (e.g., mass conservation, Darcy's law) directly into the loss function during training, ensuring that predictions are physically consistent even with limited data (Raissi et al., 2019) [82]. For CCS applications, PINNs offer several advantages: they enforce conservation laws, require fewer training samples than purely data-driven models, and provide physically interpretable solutions. Recent studies have demonstrated PINN applications for multiphase flow in porous media (Fuks and Tchelepi, 2020) [83], reservoir pressure management (Harp et al., 2021) [84], and CO_2 plume prediction. However, challenges remain: PINNs can be computationally intensive for large-scale 3D problems, and their effectiveness depends on accurate physical parameterization.

The physics of hydrodynamic trapping interactions during full-cycle CO_2 injection was systematically analyzed by Wang et al. [85]. Their numerical framework revealed that residual trapping is governed by advective transport during the injection period and becomes more significant in systems with lower permeability. Dissolution trapping operates under varying driving forces at different stages: advective transport controls dissolution during injection, while gravity-induced convection enhances dissolution in the post-injection period. Critically, the study demonstrated that trapping mechanisms are dynamically interconnected and influence each other even outside their main time scales of importance, a finding that has significant implications for ML model design, as models must capture these cross-mechanism interactions.

3.2.3. Uncertainty and Risk Assessment

Given the inherent complexity of subsurface systems, stochastic simulation techniques are often used to assess uncertainties in plume migration, providing probabilistic forecasts under multiple geological scenarios [67]. Complementary risk assessment frameworks identify potential leakage pathways, such as legacy wells or fault zones, and evaluate their possible environmental impacts [63]. The outcomes of these analyses guide the development of targeted monitoring and mitigation strategies to enhance storage security.

3.3. Pressure Monitoring and Pore Pressure Management

Pressure monitoring is vital for maintaining reservoir integrity during both the injection and storage phases. Abnormal pressure buildup may indicate caprock failure, fault reactivation, or CO_2 plume escape, all of which pose significant safety concerns. Hence, continuous pressure monitoring is a cornerstone of secure storage operations [73].

3.3.1. The Role of Pore Pressure in Reservoir Stability

Pore pressure, the pressure of formation fluid within reservoir pores, is a critical parameter affecting wellbore stability, fault reactivation potential, and safe injection pressure management. As pore pressure increases during CO_2 injection, the effective stress on the rock matrix decreases, potentially leading to rock failure or fault slip if critical thresholds are exceeded [86].

The coupling between pore pressure and in situ stress has significant implications for CCS operations. According to poroelastic theory, changes in pore pressure (ΔPp) induce corresponding changes in horizontal stresses, given by $\Delta\sigma h = [\alpha(1 - 2\nu)/(1 - \nu)]\ \Delta Pp$, where α is Biot's constant and ν is Poisson's ratio [87]. This coupling effect means that pore pressure increase during CO_2 injection causes horizontal stresses to rise, which can alter the stress regime—potentially transforming a normal faulting environment into a strike-slip or reverse faulting regime. Such changes may bring previously stable faults closer to failure [88].

The critical pore pressure for fault reactivation can be estimated from in situ stresses (S_1, S_3) and the frictional coefficient of discontinuities (μ). A higher critical pore pressure is preferred, as it allows greater CO_2 storage volume before triggering shear along discontinuities [89]. Reservoir size and boundary conditions also influence pore-pressure buildup; smaller reservoirs with closed boundaries experience higher pressure increases and greater fault reactivation risk compared to larger reservoirs with open boundaries [88].

3.3.2. Continuous Monitoring

Reservoir pressure is monitored through distributed sensor systems installed at various depths and locations within the storage formation. Real-time pressure data provide insight into spatiotemporal reservoir behavior and plume migration trends [90]. When coupled with machine learning algorithms, these datasets enable automatic anomaly detection

and early-warning systems to identify irregular patterns or operational risks [47]. Modern monitoring approaches include downhole pressure gauges, seismic monitoring, and integrated risk management systems that combine mechanistic models with continuous monitoring data for real-time leakage detection and mitigation decision support [91].

3.3.3. Data Analysis and Interpretation

Machine learning models analyze large volumes of pressure data to identify abnormal pressure gradients and potential leakage events. ANNs and support vector regression (SVR) have demonstrated superior performance in interpreting sensor readings and improving the fidelity of dynamic reservoir simulations [20,50]. Pressure data also serve as essential calibration inputs for reservoir models, enhancing their predictive accuracy for plume migration, injection efficiency, and storage capacity [26].

3.3.4. Response and Mitigation

Abnormal pressure readings require immediate operational response, which may involve reducing injection rates, altering well configurations, or temporarily halting injection operations. Rapid execution of these response strategies is essential to mitigate environmental and operational risks, preserve storage integrity, and ensure long-term project performance [54]. Effective mitigation strategies include controlled injection rates, automated pressure management systems, regular wellbore integrity assessments, and geomechanical modeling to predict the impact of changing pore pressures on reservoir stability [92,93].

Active pressure management through Downhole Water Sink (DWS) technology provides a powerful mitigation strategy for reservoir overpressure during CO_2 injection. Abdulwahab et al. [94] demonstrated that DWS extraction reduced average reservoir pressure by approximately 1100 psi, from 6150 psi to 5050 psi, thereby maintaining pressures safely below the fracture gradient (6750 psi) and mitigating risks of caprock fracturing and fault reactivation. This pressure reduction enabled safer, more continuous CO_2 injection operations while improving long-term storage security. The study showed that DWS-assisted configurations trapped 586,159 additional tons of CO_2 compared to no-DWS cases, confirming that pressure management directly enhances trapping capacity.

3.4. Robust Optimization Under Geological Uncertainty

Geological uncertainty, variations in porosity, permeability, and other reservoir properties, poses a significant challenge for CCS project design. Traditional optimization approaches that rely on a single "best estimate" geological model (nominal optimization) may fail to capture the range of possible outcomes and can lead to suboptimal injection strategies. Vo Thanh et al. [17] proposed a robust optimization workflow for CO_2 sequestration through WAG injection under geological uncertainties. Using 200 geological realizations of a heterogeneous fluvial sandstone reservoir in the Cuu Long Basin, Vietnam, the study compared nominal optimization (using a single P50 realization) with robust optimization (using P10, P50, and P90 realizations). The robust optimization framework integrated geological modeling (Petrel), compositional reservoir simulation (CMG-GEM), and an AI-based optimizer (CMOST) into a single automated workflow.

The key findings were:

1. The robust optimization strategy (30 days gas injection followed by 120 days water injection) achieved 15% higher total CO_2 trapping than the nominal optimization (50/100 cycle lengths)
2. Nominal optimization led to 13% enhanced total CO_2 trapping over the WAG base case, while robust optimization increased total CO_2 trapping by 28% over the base case

3. The base case, nominal optimization, and robust optimization achieved total trapping of 0.875, 1.074, and 1.278 Mt of CO_2, respectively

These results demonstrate that accounting for geological uncertainty through robust optimization is essential for maximizing storage efficiency and reducing project risks. The study also highlighted that the number of ranked geological realizations needed depends on reservoir complexity and available computational resources, a practical consideration for field applications.

Beyond WAG cycle optimization, recent research has explored advanced control strategies for real-time injection management. Alsubaih et al. [16] developed an adaptive smart injection system for CO_2 sequestration that integrates real-time monitoring with three control strategies: Proportional-Integral-Derivative (PID) control, Reinforcement Learning (RL), and Genetic Algorithm (GA)-based optimization. Using a fully 3D reservoir model with three injection wells and one legacy well simulated over 5 years of injection followed by 50 years of storage, the study demonstrated that smart injection frameworks significantly reduce leakage risks.

Key findings include:

1. Uncontrolled case: 10.2% of injected CO_2 leaked through the legacy well.
2. PID control: reduced leakage to 2.8% (72% reduction).
3. GA optimization: reduced leakage to 2.0% (80% reduction).
4. RL control: reduced leakage to 1.6% (84% reduction)

RL provided the greatest average leakage reduction and most adaptive response to changing reservoir conditions, whereas GA offered the most consistent performance across realizations. These results demonstrate that AI- and optimization-driven control can substantially enhance CO_2 storage security and operational efficiency, with direct transferability to waterflooding, enhanced oil recovery, and underground gas storage operations.

4. Post-Injection Monitoring and Leakage Detection

Post-injection monitoring is crucial for ensuring the long-term integrity and safety of geological CO_2 storage. Its primary goal is to verify that the injected CO_2 remains securely trapped within the target formation while identifying any potential leakage pathways that could pose environmental or health risks. This section presents a comprehensive overview of techniques used to monitor CO_2 trapping mechanisms, detect leakage, and assess reservoir responses following injection.

4.1. Monitoring and Evaluation of CO_2 Trapping Mechanisms

Effective Monitoring, Verification, and Accounting (MVA) ensure that injected CO_2 remains immobilized through residual, solubility, and mineral trapping mechanisms. As trapping processes evolve over time, the permanence of storage must be demonstrated using both direct and indirect measurements. Common MVA techniques include seismic imaging, geophysical logging, and pressure monitoring, which collectively characterize plume migration and transformation, while fluid sampling helps evaluate geochemical changes [73].

Prior to injection, baseline monitoring establishes the geological and hydrodynamic conditions of the storage site [74]. During injection, continuous monitoring tracks plume migration, whereas post-injection monitoring provides long-term surveillance to ensure containment. Among these methods, time-lapse (4D) seismic monitoring has proven the most reliable for imaging CO_2 distribution and trapping efficiency [95]. Additional techniques, including 4D-3C seismic acquisition, crosswell seismic tomography, and passive seismic monitoring, enhance spatial resolution and sensitivity for tracking plume evolution [96,97].

Downhole logging tools, such as time-lapse neutron, induction resistivity, and sonic logs, directly measure fluid saturation and changes in rock properties as CO_2 displaces brine in pore spaces [98]. Moreover, pressure transient analysis from multi-level observation wells delineates plume boundaries and confirms containment [99]. Sonic logs also detect mechanical alterations in the formation, assisting in the assessment of compaction or porosity variations [100]. A summary of major monitoring techniques and their applications throughout different project phases is presented in Table 4.

Table 4. Classification of CO_2 Trapping Monitoring Techniques.

Technique	Monitoring Phase	Data Type	Purpose	Reference(s)
4D Seismic Monitoring	Pre-, During, Post-Injection	Seismic Reflections	Track CO_2 plume evolution	Sambo et al. [95]
Crosswell Seismic Tomography	During Injection	Travel Time and Amplitude	High-resolution plume imaging	Paulsson [97]
Passive Seismic Monitoring	Post-Injection	Microseismic Events	Detect geomechanical changes	Verdon et al. [96]
Time-Lapse Well Logging	During, Post-Injection	Neutron, Resistivity, Sonic Logs	Determine saturation changes	Xue et al. [98]
Pressure Transient Analysis	During Injection	Pressure Data	Define plume boundaries	Jackson et al. [99]
Sonic Logging	During, Post-Injection	Elastic Wave Velocity	Detect rock alterations	Ajo-Franklin et al. [100]
Groundwater Sampling	Post-Injection	Water Chemistry	Identify geochemical changes	Ajayi et al. [101]
Atmospheric Sensing (Optical, Tracers)	Post-Injection	CO_2 Concentration	Detect surface leakage	Sun et al. [102]; Watson and Sullivan [103]
Eddy Covariance and Remote Sensing	Post-Injection	Gas Flux Data	Monitor atmospheric leakage	Verkerke et al. [104]

Beyond monitoring technique selection, the value of different monitoring data types can be quantified through expected uncertainty reduction in key risk metrics. Chen et al. [19] developed a filtering-based data assimilation procedure combined with Multivariate Adaptive Regression Splines (MARS) to design optimal monitoring strategies for GCS. The approach quantified uncertainty reduction in cumulative CO_2 leakage as a metric for monitoring value, enabling quantitative comparison of different monitoring designs. Key findings included:

1. Pressure data provide higher value of information than CO_2 saturation or temperature data
2. Simultaneous use of multiple monitoring signals reduces uncertainty more effectively than single-signal monitoring
3. The incremental benefit of additional monitoring wells diminishes beyond a certain number, suggesting an optimal monitoring network density

This quantitative framework for monitoring design represents a significant advance over qualitative approaches, enabling operators to justify monitoring investments based on expected risk reduction.

Advanced monitoring techniques have evolved significantly to address the unique challenges of CCS. Alsubaih et al. [35] provided a comprehensive review of monitoring technologies, including:

1. Four-dimensional seismic monitoring for tracking CO_2 plume migration.
2. Wireline logging for high-resolution data around injection wells.
3. Groundwater sampling to detect geochemical changes from CO_2 leakage.
4. Atmospheric monitoring using optical fiber sensors, flux chambers, and tracer gases.

5. Interferometric Synthetic Aperture Radar (InSAR) for measuring surface deformation (5–10 mm/a uplift at In Salah, Algeria).

The review emphasized that seismic methods are most effective for large-scale structural-stratigraphic trapping evaluation, while wireline logging provides critical insights for estimating structural-stratigraphic trapping mechanisms. At the Nagaoka pilot site in Japan, sonic logs detected a 28% change in shear velocity between pre- and post-CO_2 injection, while cross-hole tomography showed a 17% change in velocity, demonstrating the complementary value of multiple monitoring techniques.

Figure 6 visualizes the cost-sensitivity trade-offs among these monitoring techniques. The chart reveals that high-sensitivity techniques (crosswell tomography, downhole logging) have limited spatial and temporal coverage, while continuous techniques (pressure monitoring, atmospheric sensing) have lower sensitivity. Optimal monitoring strategies therefore combine multiple techniques to balance these trade-offs.

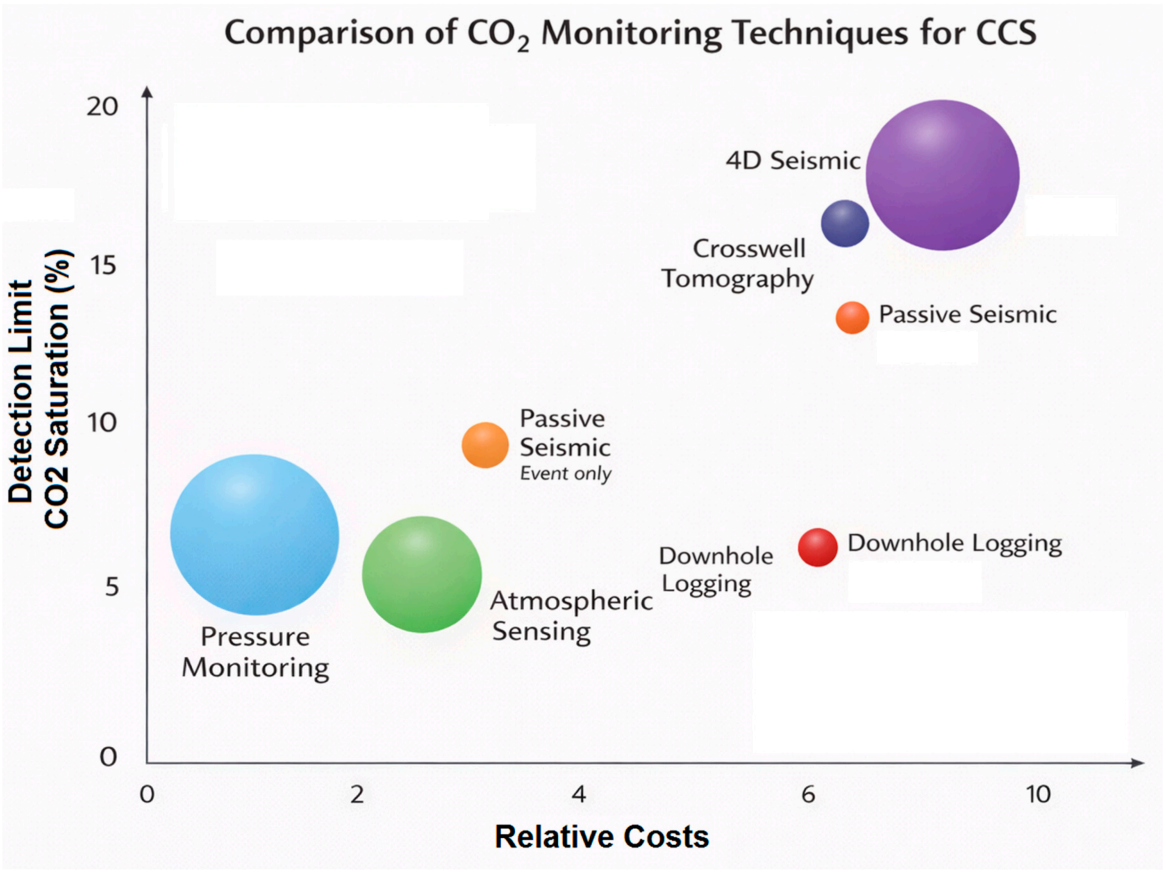

Figure 6. Cost-sensitivity analysis of CO_2 monitoring techniques for CCS. Bubble chart comparing monitoring methods by relative cost (*X*-axis), detection sensitivity (*Y*-axis, as minimum detectable CO_2 saturation), and spatial coverage (bubble size). The chart reveals fundamental trade-offs: high-sensitivity techniques (crosswell tomography, downhole logging) have limited spatial coverage and temporal frequency, while continuous techniques (pressure monitoring, atmospheric sensing) have lower sensitivity. No single technique provides complete spatiotemporal coverage at acceptable cost; optimal monitoring strategies combine multiple methods.

4.1.1. Groundwater and Atmospheric Monitoring for Leakage Detection

Upward CO_2 migration may affect shallow aquifers or reach the surface, making groundwater and atmospheric monitoring essential for early detection. Groundwater monitoring involves periodic sampling and chemical analyses to detect variations in pH, alkalinity, and trace metal concentrations caused by elevated CO_2 levels. Reactive transport

modeling at the field scale further interprets these geochemical changes and predicts potential leakage scenarios [101].

Atmospheric monitoring relies on highly sensitive systems capable of detecting minor increases in CO_2 concentration near storage sites. Optical fiber sensors, flux chambers, and tracer gas techniques are commonly employed [102,103]. Additionally, eddy covariance and remote sensing methods enable continuous surface flux monitoring and rapid leakage detection.

4.1.2. Experimental Investigations of CO_2 Trapping Mechanisms

Petrophysical Characterization

Understanding rock–fluid interaction is vital for modeling CO_2 flow, distribution, and trapping efficiency. Petrophysical parameters such as porosity, permeability, saturation, capillary pressure, and relative permeability are typically determined through Routine Core Analysis (RCAL) and Special Core Analysis (SCAL) [105,106]. These measurements support accurate predictions of injectivity and storage performance.

Pore-Scale Visualization

Advanced imaging techniques, including microfluidics, MRI, and micro-CT scanning, provide detailed visualization of multiphase flow and pore-scale trapping mechanisms. These approaches reveal how capillary forces, wettability, and pore geometry influence residual trapping efficiency [107–109].

CO_2–Fluid–Rock Interactions

Experimental studies on fluid–fluid and fluid–rock interactions yield critical insights into chemical trapping. Laboratory experiments evaluate mineralogical alterations and the resulting changes in porosity and permeability due to geochemical reactions induced by CO_2 injection. These findings contribute to risk assessment and long-term storage evaluation [81,110].

Adsorption Phenomena

CO_2 adsorption onto mineral surfaces plays a major role in shale and coal reservoirs. Gravimetric, volumetric, manometric, and chromatographic methods are used to quantify adsorption capacities and kinetics [111,112]. These experimental data are essential for modeling CO_2 retention and estimating effective storage volumes in nanoporous media. A detailed comparison of experimental trapping methods and parameters is presented in Table 5.

Table 5. Summary of Experimental Techniques for CO_2 Trapping Mechanisms.

Method	Focus	Measured Properties	Reference
Routine Core Analysis (RCAL)	Petrophysical properties	Porosity, permeability, fluid saturation	Tiab and Donaldson [105]; Liu and Grana [106]
Special Core Analysis (SCAL)	Capillary pressure and relative permeability	Wettability, capillary pressure curves	Tiab and Donaldson [105]; Liu and Grana [106]
Microfluidics	Pore-scale flow visualization	Capillary trapping, flow pathways	Jiang et al. [107]
Magnetic Resonance Imaging (MRI)	Dynamic imaging of fluid flow	Fluid saturation, distribution	Soong et al. [108]

Table 5. *Cont.*

Method	Focus	Measured Properties	Reference
Micro-Computed Tomography (micro-CT)	3D pore structure imaging	Pore geometry, residual trapping	De et al. [109]
Gravimetric Method	CO_2 adsorption capacity	Adsorbed CO_2 mass	Petrovic et al. [111]
Volumetric Method	Adsorption isotherms	Gas volume at set pressure/temp	Petrovic et al. [111]
Manometric Method	Gas–solid interactions under pressure	Adsorption pressure response	Abdulkareem et al. [112]
Chromatographic Method	Adsorption kinetics	Breakthrough curves, retention times	Abdulkareem et al. [112]

4.2. Anomaly Detection

Well integrity monitoring is a critical aspect of GCS, as poorly maintained or abandoned wells may act as leakage conduits. Continuous subsurface surveillance enables the early detection of anomalies, helping to mitigate leakage risks and improve understanding of CO_2 plume migration and containment efficiency [113]. Anomalies typically fall into three categories:

1. Shift outliers indicating gradual distribution changes,
2. Transient shifts representing short-term deviations, and
3. Point outliers caused by geological changes, equipment faults, or fluid migration.

Accurate identification of these anomalies is essential for maintaining operational and structural integrity. Recent advances in deep learning have greatly enhanced anomaly detection in complex, high-dimensional time-series data. Govindan et al. [114] applied Independent Component Analysis (ICA) and Impulse Response Functions (IRF) to remote sensing data to identify surface leakage. Meanwhile, Zhang et al. [67] proposed a hybrid CNN–BiLSTM model that achieved superior accuracy for bottom-hole pressure anomaly detection.

Other frameworks include DeepSense [115] and feedforward neural networks for sensor-based anomaly classification [116]. Spatial outlier detection methods such as Subspace Local Outlier Factor (SLOF) [117] and frequency-based analyses [118] have also proven useful. A particularly robust hybrid approach integrates LSTM autoencoders with the Isolation Forest (IF) algorithm, which is trained on stochastic geological model realizations. This combination effectively detects abnormal patterns under uncertainty, improving interpretability and decision support. A summary of key deep learning methods for anomaly detection is presented in Table 6.

Recent advances in deep learning architectures have further improved anomaly detection performance. Zhong et al. [66] developed a ConvLSTM-based framework for real-time anomaly detection using pressure sensor data, achieving high accuracy in detecting irregular pressure signals indicative of potential leakage. The ConvLSTM architecture's ability to capture both spatial and temporal features makes it particularly suitable for CCS monitoring applications where pressure transients propagate through heterogeneous formations.

Zhang et al. [67] proposed a hybrid CNN-BiLSTM model that achieved superior accuracy for bottom-hole pressure anomaly detection. The hybrid architecture combines convolutional neural networks (CNNs) for feature extraction with bidirectional long short-term memory (BiLSTM) networks for sequential pattern recognition. This combination enables the model to capture both local pressure anomalies and longer-term temporal trends, reducing false positive rates compared to single-architecture approaches.

Table 6. Deep Learning Models for Anomaly Detection in CCS.

Model/Algorithm	Type	Key Features	Reference(s)
ConvLSTM	Deep Learning	Real-time anomaly detection using pressure sensor data	Zhong et al. [66]
ICA + IRF	Remote Sensing	Surface leakage detection via signal decomposition	Govindan et al. [114]
CNN-BiLSTM	Hybrid Deep Learning	Sequential pressure anomaly prediction in BHP data	Zhang et al. [67]
DeepSense	Deep Learning	General anomaly recognition framework	Bakhshian and Romanak [115]
Feedforward Neural Network	Neural Network	Classification of abnormal patterns in sensor data	Sinha et al. [116]
SLOF	Outlier Detection	Spatial outlier recognition using local factor analysis	Xin et al. [117]
Sinusoidal Pattern Detection	Frequency Analysis	Frequency-based anomaly detection	Min et al. [118]

4.3. Risk Assessment Framework for Geologic Sequestration

Geologic CO_2 sequestration entails a range of physical, chemical, and operational risks, with leakage posing the greatest concern. Migration of CO_2 into overlying formations or to the surface can lead to environmental contamination, health hazards, and regulatory challenges. Effective risk assessment depends on a comprehensive understanding of formation heterogeneity, fluid–rock interactions, and CO_2 behavior over time. The three major risk categories, environmental, health and safety, and economic, are summarized in Table 7.

Table 7. Risk Categories in Geological CO_2 Sequestration.

Risk Category	Potential Impacts	Mitigation Strategies
Environmental	Leakage into atmosphere or aquifers, induced seismicity	Proper site selection, injection control, long-term monitoring
Health and Safety	Asphyxiation, toxic exposure (e.g., H_2S), operational accidents	Gas detection systems, emergency protocols
Economic	Cost overruns, leakage liability, insurance, tax penalties	Cost–benefit analysis, regulatory compliance, project insurance

4.3.1. Environmental Risks

Even minimal atmospheric leakage undermines sequestration goals, potentially causing CO_2 accumulation in soils or migration into unintended strata [119]. Offshore leakage may lower oceanic pH and disrupt marine ecosystems. Additionally, displacement of brine or hydrocarbons can impact nearby production zones or contaminate freshwater aquifers. Excessive injection pressure may induce seismicity, while mineral precipitation can reduce reservoir permeability despite contributing to long-term mineral trapping.

4.3.2. Health and Safety Risks

CO_2 accumulation in confined spaces can displace oxygen and cause asphyxiation. Concentrations above 3% are hazardous, while levels exceeding 10% are potentially

fatal [120]. Infrastructure components such as pipelines and compressors pose additional hazards if not properly maintained. When H_2S is co-injected with CO_2, toxicity risks increase substantially [121].

4.3.3. Economic Risks

The economic feasibility of CCS projects remains a major concern. Retrofitting power plants for CO_2 capture can increase electricity production costs by 30–65%, depending on the technology used [122]. High capital and operational costs, coupled with potential liability for leakage or reservoir failure, represent significant risks. Unexpected geological faults or poor injectivity may lead to financial losses or forfeiture of carbon credits. In cases of contamination, remediation and litigation costs further elevate risks. Robust geological characterization, economic modeling, and mitigation strategies are therefore essential for long-term project success.

4.4. CO_2 Leakage and Fault Reactivation

Leakage represents the principal failure mode in CCS operations. Ideally, a well-engineered reservoir with an intact caprock should contain CO_2 for millennia. However, faults, fractures, or compromised wells can allow upward migration [119]. Leakage typically occurs locally through narrow vertical pathways or abandoned wells [121]. For CCS to effectively offset emissions, leakage rates must remain below 0.001–0.01% per year [122].

4.4.1. Fault Reactivation Mechanisms

Fault reactivation is a significant concern during CO_2 injection, as increased pore pressure reduces effective normal stress on fault planes, potentially inducing slip. The likelihood of reactivation depends on the faulting regime, Poisson's ratio, and the non-uniform nature of reservoir deformation. Figure 7 illustrates the fault reactivation mechanism in two panels. Panel (a) shows a cross-section of a fault intersecting the storage reservoir and caprock; CO_2 injection increases pore pressure (ΔPp), which propagates along the fault plane. Panel (b) presents a Mohr circle representation of the stress evolution: initial effective stresses (σ_1', σ_3') are shown in blue; pore pressure increase shifts the circle leftward (red dashed), reducing effective stress and potentially bringing the fault to failure (touching the failure envelope). The critical pore pressure for reactivation depends on in situ stresses (S_1, S_3) and the fault friction coefficient (μ).

Research by Lele et al. [123] demonstrates that injection-induced fault slip is more likely in layers other than the reservoir for normal and strike-slip faulting regimes, but within the reservoir layer for reverse faulting, due to Poisson's ratio effects. Fault slip can localize in either the layer above or below the reservoir depending on the faulting regime and well placement relative to the fault.

Guglielmi et al. [124] conducted field-scale fault reactivation experiments demonstrating aseismic leakage in caprock analogs, with direct implications for CO_2 sequestration safety. Their findings highlight that fault reactivation can occur without detectable seismic events, emphasizing the need for continuous monitoring of pressure and deformation.

A critical aspect often overlooked in leakage risk assessment is the role of legacy and orphaned wells. Alsubaih et al. [125] documented that over 225,000 orphaned wells exist in the United States, with estimates suggesting up to 3.9 million wells nationwide emitting approximately 3.2 Tg of methane annually. These wells pose significant risks to CCS operations, as they can serve as unintended leakage pathways for stored CO_2. The study employed a Random Forest regressor to predict potential orphan well locations based on historical data, enabling more targeted monitoring and remediation efforts.

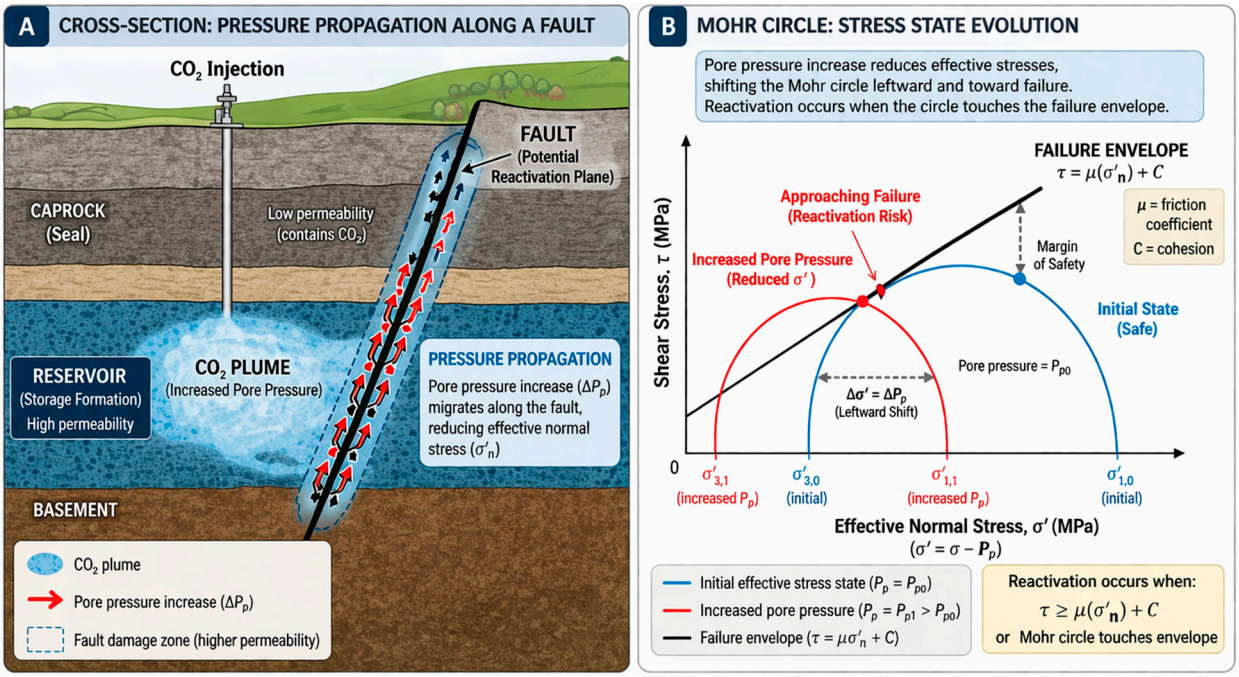

Figure 7. Conceptual diagram of fault reactivation risk during CO_2 injection. (**A**) Cross-section showing a fault intersecting the storage reservoir and caprock. CO_2 injection increases pore pressure (ΔPp), which propagates along the fault damage zone (higher permeability), reducing effective normal stress on the fault plane. (**B**) Mohr circle representation of stress evolution. Initial effective stresses (σ_1', σ_3') are shown in blue; pore pressure increase shifts the circle leftward (red dashed line) by $\Delta\sigma' = \Delta Pp$, reducing effective stress. Reactivation occurs when the circle touches the failure envelope ($\tau = \mu\sigma' n + C$, where μ is the friction coefficient and C is cohesion). The purple shaded area represents the margin of safety; the green shaded area indicates approaching failure. Understanding these mechanisms is essential for maintaining injection pressures below safety thresholds.

For quantitative leakage risk assessment, Alsubaih et al. [16] compared three modeling philosophies for brine leakage through legacy wells:

1. Reservoir-scale analytical solution [126]: predicts gradual leakage (~1.7 bbls/day after 1000 days).
2. Semi-analytical pressure-transient model [127]: predicts higher rates (>8 bbls/day after 1000 days).
3. Mechanistic wellbore-scale model (new): yields damage-dependent outcomes (0.2–0.4 bbls/day for moderate-severe cement damage; ~3.5 bbls/day for open-channel conditions).

The comparison demonstrates that model choice and physics assumptions drive order-of-magnitude differences in predicted leakage rates, emphasizing the need for fit-for-purpose model selection in CCS risk assessment.

4.4.2. Natural Hazards and Caprock Integrity

Natural hazards, such as seismic events, may compromise caprock integrity, particularly in formations with high-permeability faults. Using InSAR, Aker et al. [128] detected surface deformation at the In Salah site in Algeria, linking pressure-induced uplift to subsurface leakage potential. Finite element modeling confirmed the correlation between injection strain and stress redistribution. Formation permeability and porosity are key factors influencing vertical migration [129], while elevated temperatures in deep reservoirs can enhance CO_2 mobility [130].

Modern probabilistic simulations and 3D seismic mapping now enable precise leakage risk assessment [131–133]. Ultimately, long-term storage integrity depends on rigorous site

selection, advanced monitoring, and a robust regulatory framework. When integrated with sensor and simulation data, machine learning-based leakage prediction tools can greatly improve early detection and response, ensuring safe and sustainable CO_2 storage systems.

4.5. Formation Water Salinity and CO_2 Solubility

The solubility of CO_2 in formation brine is essential for ensuring the success of CCS projects, as CO_2 dissolution stabilizes storage and prevents upward migration, ensuring long-term containment [134]. Pressure is a primary factor affecting solubility, increasing CO_2 absorption according to Henry's Law [135]. High-pressure conditions found in deep saline reservoirs are ideal for CO_2 storage because they enhance solubility.

However, temperature reduces CO_2 solubility by weakening the interaction between gas and water molecules [136]. Salinity introduces another significant factor through the "salting-out effect," where dissolved salts limit water's capacity to retain CO_2 [137]. Sites with high total dissolved solids (TDS) require special attention, as high salinity can significantly impact storage efficiency [138].

Geochemical models are essential for predicting CO_2 solubility and optimizing CCS operations. Figure 8 illustrates CO_2 solubility in brine as a function of pressure, temperature, and salinity, calculated using the Duan and Sun [135] thermodynamic model. The Duan and Sun model offers high accuracy for CO_2-water systems but struggles with complex brine compositions [139]. Machine learning approaches have been developed to improve solubility predictions; for example, Pan et al. [138] developed a modified version of Duan's model for real brines that achieved a 5.11% deviation compared to 12.10% with the original model.

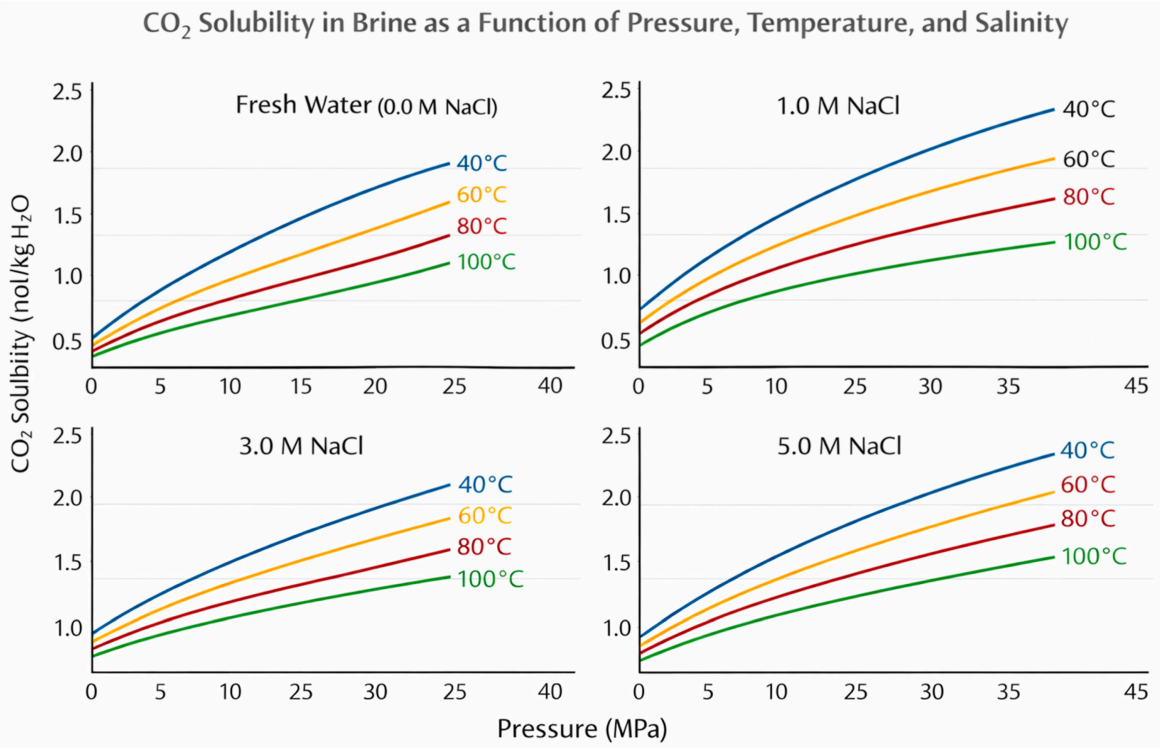

Figure 8. CO_2 solubility in brine as a function of pressure, temperature, and salinity, calculated using the Duan and Sun [135] thermodynamic model. Higher pressures enhance solubility following Henry's Law, as shown by the upward trend across all temperature and salinity conditions. Elevated temperatures reduce solubility by weakening gas-water intermolecular interactions. Increased salinity further reduces solubility through the "salting-out" effect, where dissolved ions compete with CO_2 molecules for water solvation shells. These relationships are critical for estimating storage capacity in deep saline aquifers and optimizing injection strategies.

CO_2 injection not only influences solubility but also affects the chemical and physical properties of reservoirs. It causes the pH of formation water to drop from approximately 7.4 to 6.5, which alters the chemical environment and leads to mineral precipitation, such as carbonates and silicates [140]. These chemical changes can impact both porosity and permeability. For example, Liu et al. [141] developed a reactive transport model showing that CO_2-water-rock reactions, though minimally altering shale porosity (<1%), significantly impact CH_4 production and CO_2 storage by controlling reservoir pressure and CO_2 migration. Sensitivity analysis revealed that high pressure, low permeability, and low injection rates intensify these geochemical effects, while factors promoting CO_2 migration increase leakage risks.

Advanced machine learning techniques have been developed to improve CO_2 solubility predictions. Menad et al. [9] developed multilayer perceptron (MLP) and radial basis function neural network (RBFNN) models optimized by Levenberg–Marquardt, Genetic Algorithm (GA), Particle Swarm Optimization (PSO), and Artificial Bee Colony (ABC) algorithms. Using 570 experimental data points spanning pressures up to 1400 bar, temperatures up to 723.15 K, and NaCl molality up to 6.14 mol/kg, the RBFNN-ABC model achieved the highest accuracy with RMSE = 0.0289 and R^2 = 0.9967. This model significantly outperformed existing thermodynamic models (achieved R^2 = 0.9301 on the same dataset) and was made available as an Excel-based calculator tool for practical application. Yang et al. [142] used experimental data from literature train and predict CO_2 solubility by four machine learning models: support vector regression (SVR), extreme gradient boosting (XGBoost), random forest (RF), and multilayer perceptron (MLP). Among four models, the XGBoost model has the best predictive performance, with an R^2 of 0.9838.

Al-qaness et al. [143] further advanced this approach by developing an optimized ANFIS model using a hybrid Aquila Optimizer and Salp Swarm Algorithm (AOSSA). Using 6810 simulation samples with 8 input features (porosity, permeability, thickness, salinity, depth, residual gas saturation, injection rate, and time-elapse), the AOSSA-ANFIS model achieved RMSE values of 0.15001 and 0.06904 for residual and solubility trapping indices, respectively. The study demonstrated that hybrid optimization algorithms significantly enhance the predictive performance of conventional ANFIS models, and the proposed AOSSA-ANFIS outperformed seven other optimized ANFIS variants, including those using GA, PSO, and MFO.

4.6. Digital Twin and Artificial Intelligence for Well Integrity Monitoring

The digital transformation of the oil and gas industry has introduced powerful tools for well integrity management. Alsubaih et al. [35] provided a comprehensive review of digital twin technologies for well integrity across conventional, unconventional, and storage wells. A digital twin functions as a dynamic, synchronized virtual representation of a physical well asset and its surrounding environment, integrating real-time sensor data with sophisticated simulation models.

Key components of a well integrity digital twin include:

1. Static data: as-built well designs, casing specifications, formation properties, cementing job parameters.
2. Dynamic data: real-time pressure, temperature, flow rates, distributed temperature sensing (DTS), distributed acoustic sensing (DAS).
3. Physics-based models: simulating multiphase flow, heat transfer, thermo-hydro-mechanical-chemical (THMC) stresses.
4. AI/ML modules: predictive maintenance tools, anomaly detection systems, remaining useful life (RUL) forecasts.

The integration of machine learning with digital twins enables predictive maintenance, early failure detection, and lifecycle risk management. ML models trained on historical and real-time data can identify subtle anomalies that may precede failure, predict RUL of critical components, optimize inspection schedules based on predicted risk, and automatically generate alerts for potential integrity issues.

Field applications of digital twins have demonstrated significant value in high-risk operations such as CCS, deepwater production, and geothermal energy extraction. The technology enables operators to evaluate well integrity status, simulate leak evolution, predict casing fatigue, assess the risk of sustained casing pressure (SCP), model cement degradation, and test remediation scenarios, all without physical intervention. As the energy transition accelerates, digital twins will become essential for ensuring secure and scalable deployment of subsurface storage solutions.

4.7. Deep Learning for History Matching with 4D Seismic Data

History matching, the process of calibrating geological models to observed data, is essential for reducing uncertainty in CCS performance predictions. However, traditional history matching approaches are computationally expensive, often requiring thousands of high-fidelity simulations. Deep learning surrogate models offer a promising solution. Wang and Durlofsky [144] introduced a deep learning framework for history matching CO_2 storage with 4D seismic and monitoring well data. The framework employs two fit-for-purpose surrogate models: a 3D U-Net for predicting interpreted (coarse-scale) 4D seismic saturation fields and a 1D U-Net for predicting monitoring well data. Both networks accept high-resolution geomodels as input and have multiple output channels corresponding to different time steps.

Key features and findings include:

1. Training efficiency: The two specialized networks required only 2.25 h of GPU training, compared to tens of hours for single-network alternatives
2. Prediction speed: Function evaluations require less than 0.1 s, enabling efficient Markov chain Monte Carlo (MCMC) history matching
3. Uncertainty quantification: The hierarchical MCMC procedure produced posterior distributions for both metaparameters (e.g., mean log-permeability, standard deviation) and fine-scale geomodel realizations
4. Value of 4D seismic data: Incorporating 4D seismic data (even binary plume location data) significantly reduced posterior uncertainty in key geomodel parameters compared to using monitoring well data alone
5. Practical insight: The study demonstrated that seismic data providing only plume location (presence/absence of CO_2 above a threshold) still provided substantial value, though interpreted saturation data yielded slightly better uncertainty reduction

This framework represents a significant advance in CCS data assimilation, enabling quantitative assessment of the value of different data types and providing a computationally tractable approach to uncertainty quantification in large-scale storage projects.

5. Case Studies and Success Stories

The applications of machine learning (ML) in carbon capture and storage (CCS) have significantly improved operational efficiency, site safety, and monitoring accuracy. This section highlights several notable international case studies that demonstrate the integration of ML techniques across different CCS stages, including site characterization, capacity estimation, storage modeling, anomaly detection, and risk management. Each case illustrates unique benefits, technical innovations, and lessons learned.

5.1. Illinois Basin—Decatur Project (USA)

The Illinois Basin–Decatur Project (IBDP) serves as a leading example of ML utilization in site selection and storage capacity estimation. The GeoSeq Consortium in collaboration with the U.S. Department of Energy (DOE) [145] executed the project, designed to inject one million metric tons of CO_2 per year into the Mt. Simon Sandstone Formation.

Traditionally, site selection depended on core sampling and geological surveys. In contrast, ML facilitated rapid processing of seismic, petrophysical, and reservoir datasets. Deep learning models such as Convolutional Neural Networks (CNNs) and Artificial Neural Networks (ANNs) were applied to identify optimal injection zones and evaluate formation suitability [146].

Formation regions were automatically categorized into secure, moderate, and unsafe zones based on permeability and pore-pressure parameters [147]. By 2017, over one million tons of CO_2 had been successfully injected with no recorded leakage, confirming the project's long-term storage integrity. The ML-enhanced models also improved risk reduction and predictive reliability [148].

5.2. Boundary Dam CCS Project (Canada)

The Boundary Dam Project in Saskatchewan, Canada, represents one of the world's first commercial-scale CCS applications at a coal-fired power plant. Operational since 2014, it was designed to capture 90% of CO_2 emissions, equivalent to roughly one million tons annually.

Despite early challenges, such as fly ash buildup, surface leakage, and inconsistent capture rates (ranging from 400,000 to 800,000 tons per year), the project successfully demonstrated the role of ML in performance optimization. Hybrid electrostatic precipitators, controlled by ML-based optimization algorithms, were introduced to improve particulate filtration prior to chemical absorption, thereby reducing downtime and enhancing system reliability.

The project highlights ML's effectiveness in predictive maintenance, fault diagnosis, and process optimization, offering a model for integrating intelligent control systems into CCS operations [149,150].

5.3. Gorgon CCS Project (Australia)

The Gorgon Project, operated by Chevron and its partners, is among the largest CCS initiatives globally, with an intended storage target of up to four million tons of CO_2 per year from natural gas operations on Barrow Island, Australia [151].

Initially, the project faced technical issues, including reservoir heterogeneity, injection pressure anomalies, and component malfunctions, which limited its ability to meet regulatory requirements [152]. ML algorithms were subsequently implemented to refine geological models and optimize injection strategies. Supervised learning and geostatistical kriging techniques were employed to update spatial models of plume dynamics, improving prediction accuracy and reducing uncertainty [153].

In parallel, predictive maintenance algorithms, trained on sensor data, reduced equipment failure rates. Although early setbacks delayed full operation, the project underscored ML's scalability for large, complex CCS systems and the importance of adaptive learning integration in real-time reservoir management [154].

5.4. Sleipner CO_2 Storage Project (Norway)

The Sleipner Project, operated by Equinor, stands as the world's longest-running offshore CCS operation, with over 20 million tons of CO_2 injected into the Utsira Formation since 1996 [149,155].

ML applications enhanced geophysical monitoring by integrating artificial neural networks with time-lapse seismic and electromagnetic data [147]. Repeat seismic and gravity surveys improved plume tracking accuracy, while ML algorithms provided more sensitive detection of plume evolution and reduced false positives in leakage identification [156]. The Sleipner experience demonstrates how ML can strengthen offshore monitoring, refine geophysical interpretation, and ensure storage integrity even under harsh marine conditions [157].

5.5. Quest CCS Project (Canada)

The Quest Project, operated by Shell in Alberta, Canada, aims to store over 1.2 million tons of CO_2 annually from the Athabasca Oil Sands operations [158]. Since commencing in 2015, the project has achieved a 35% reduction in CO_2 emissions from associated facilities.

ML has been integrated into subsurface modeling, injection optimization, and leak risk analysis. Reinforcement learning algorithms were used to optimize injection scheduling and maximize storage efficiency [159]. Despite early financial and operational challenges, continuous ML-driven performance improvement has proven the commercial viability of intelligent CCS systems. ML tools were also applied for surface risk assessments, cost forecasting, and real-time operational management. Quest thus serves as a blueprint for future CCS deployments, showcasing how AI can enhance decision-making, efficiency, and long-term environmental compliance.

5.6. Teapot Dome CO_2 Storage Project (Wyoming, USA)

The Teapot Dome Field in Wyoming, also known as Naval Petroleum Reserve #3 (NPR-3), has been selected by the U.S. Department of Energy for field-scale CO_2 storage research. The Tensleep Sandstone formation, at an average depth of 1657 m, provides suitable pressure and temperature conditions for supercritical CO_2 storage.

Abdulkhaleq et al. [56] conducted an optimization study using RBF-NN proxy modeling to maximize CO_2 trapping efficiency. Three injection scenarios were evaluated: vertical injectors (VI), vertical injectors with water sink (VIWS), and horizontal injectors with water sink (HIWS). The VIWS scenario proved most effective, achieving a total trapping index of 83.5% with 44,100 tons of CO_2 stored and only 1.3% leakage. Sensitivity analysis revealed that the number of open wells and maximum bottomhole injection pressure were the most influential parameters affecting trapping efficiency. This case study demonstrates that proxy-based optimization can significantly enhance CO_2 storage performance even in geologically challenging formations with poor porosity (average 8%) and permeability (average 10.27 mD). The methodology is transferable to other saline aquifers with similar reservoir characteristics.

5.7. Orphaned and Abandoned Wells: Implications for CCS Site Selection

A critical challenge for CCS deployment in the United States is the presence of millions of orphaned and abandoned wells that could serve as leakage pathways. Alsubaih et al. [125] analyzed state-level data to estimate documented orphan wells at 225,287, significantly higher than the EPA's previous estimate of 123,000 wells. The study employed a Random Forest regressor to predict the locations of undocumented orphan wells, enabling more targeted monitoring and remediation.

Key findings for CCS site selection include:

1. Over 4.6 million people live within 1 km of orphaned wells, highlighting public health risks
2. Methane emissions from inactive wells amount to 7–20 million metric tons CO_2 equivalent annually

3. The depth distribution of orphan wells overlaps with typical CCS injection depths (2500–20,000 ft)
4. States with high orphan well density (Pennsylvania, Texas, Oklahoma, Ohio) require careful site screening

The study emphasizes that CCS projects must conduct rigorous legacy well screening and, where necessary, re-abandonment campaigns before operations can safely commence. This represents a significant component of overall project cost and risk that is often underestimated in early-stage CCS planning.

Collectively, these international case studies demonstrate how ML integration across the CCS lifecycle, from site evaluation and reservoir modeling to anomaly detection and risk management, yields measurable improvements in safety, cost-efficiency, and sustainability. A comparative overview of these projects, including AI methods used, outcomes, and lessons learned, is provided in Table 8.

While Table 3 provided a method-focused comparison of ML applications across CCS stages, Table 8 offers a project-focused synthesis of real-world case studies. The two tables are complementary: Table 3 emphasizes algorithmic approaches and their benefits/challenges, whereas Table 8 emphasizes project outcomes, key challenges, and lessons learned from field deployment. Where projects appear in both tables (e.g., Illinois Basin-Decatur, Sleipner), the information is intentionally presented at different levels of granularity, Table 3 summarizes the ML methods used, while Table 8 provides operational context and project-specific outcomes.

Table 8. Summary of CCS Case Studies with AI Integration.

Project	Location	AI Application	Key Challenges	Outcomes	Reference(s)
Illinois Basin—Decatur Project (IBDP)	Illinois, USA	ML for site selection, geological data analysis, permeability and porosity modeling	Subsurface uncertainty, large data processing	Improved site characterization, reduced search time and cost, enhanced suitability prediction	Zhang et al. [145]; Pradoo et al. [146]
Boundary Dam	Saskatchewan, Canada	Hybrid AI systems for fly ash control, reliability optimization	Fly ash accumulation, frequent downtimes, high operational cost	Improved plant stability, emission reduction (70–80%), optimized particle capture	Giannaris et al.; Pradoo et al. [146]
Gorgon CCS Project	Barrow Island, Australia	Pressure analysis and reservoir monitoring with ML	Geological complexity, low injection performance, high cost	Enhanced modeling; however, storage fell short of targets, triggering need for technology reassessment	Timperley [152]; IEEFA
Sleipner Project	North Sea, Norway	AI-enhanced seismic and EM data analysis, CO_2 flow simulation	Deep reservoir monitoring, subtle leak detection in marine setting	Over 20 Mt stored safely; improved precision in CO_2 movement tracking via neural networks	Al-Khudhairy and Løseth [147]; Nooner and Vasco [156]

Table 8. *Cont.*

Project	Location	AI Application	Key Challenges	Outcomes	Reference(s)
Quest Project	Alberta, Canada	ML applied for injection monitoring and optimization	Budget overrun, leakage risk, environmental scrutiny	Significant CO_2 reduction (35%); demonstrated economic and technical viability of CCS	[158,159]
Teapot Dome Field	Wyoming, USA	Simulation and ML Algorithms	Active Aquifer	Total trapping index of 83.5% with 44,100 tons of CO_2 stored and only 1.3% leakage	Abdulkhaleq et al. [56]
Orphaned and Abandoned wells	Pennsylvania, Texas, Oklahoma, Ohio	CCS deployment	Leakage Pathways	rigorous legacy well screening	Alsubaih et al. [125]

5.8. South Rumaila Field Integrated CO_2 Storage Optimization (Iraq)

The South Rumaila oil field in southern Iraq has served as a testbed for integrated ML-assisted CO_2 storage optimization. Multiple studies have evaluated the combination of Downhole Water Sink (DWS) technology, Huff and Puff (HnP) injection, and machine learning-based optimization in both depleted hydrocarbon reservoirs and fully water-saturated aquifers [57,58,79,94].

Key Findings:

NN-RBF Proxy Performance: RBF-NN surrogate models achieved R^2 = 0.982–1.000 for predicting CO_2 trapping efficiency, enabling rapid optimization of injection strategies without compromising accuracy [57,58].

DWS Pressure Management: DWS extraction reduced average reservoir pressure by ~1100 psi, maintaining pressures below the fracture gradient and enabling safer, more continuous injection operations [94].

Optimization Improvements: Well location optimization increased CO_2 storage by 21.2% (3.3 → 4.0 Mt), while flow rate optimization achieved 15.92 Mt CO_2 trapped with LI = 3.38% [94].

NN-RBF vs. PSO: NN-RBF-based optimization outperformed PSO in solution stability, computational efficiency, and balanced performance across multiple objectives (CO_2 storage, trapping efficiency, and leakage reduction) [57].

DWS-HnP Integration: Combined DWS and Huff-and-Puff injection achieved TTI = 0.99 (99% trapping) and LI = 0.002 (0.2% leakage), demonstrating near-complete containment with active pressure management [94].

These studies demonstrate that ML-assisted optimization with DWS pressure management provides a scalable, computationally efficient framework for enhancing CO_2 storage security in mature reservoirs. The methodology is transferable to other depleted hydrocarbon reservoirs and saline aquifers with similar geological characteristics.

6. Discussion

This section synthesizes the key findings of this review, critically evaluates the evidence presented, compares conflicting results across studies, addresses the limitations of reviewed methods, and identifies open knowledge gaps that remain after this comprehensive synthesis. The discussion is organized around four themes: (1) synthesis of reviewed evidence; (2) comparison of conflicting results; (3) critical evaluation of limitations; and (4) open knowledge gaps and future research priorities.

6.1. Synthesis of Reviewed Evidence

Across the CCS lifecycle, several overarching patterns emerge from the reviewed literature that transcend individual studies and methodological approaches.

6.1.1. Consistent Performance Hierarchy of ML Algorithms

A consistent finding across multiple independent studies is the performance hierarchy of ML algorithms for CO_2 trapping prediction. Vo Thanh et al. [15] demonstrated that XGBoost consistently outperforms RF and SVR, achieving R^2 = 0.9993 and RMSE = 0.0041. Safaei-Farouji et al. [55] independently confirmed this ranking, finding RF > ANFIS > RBF > ET for residual and solubility trapping. Vo Thanh and Lee [15] further showed that GPR achieved R^2 = 0.992, outperforming SVM and RF. Collectively, these studies establish a robust performance hierarchy: XGBoost $\geq$ GPR > RF > ANN > SVR, with the specific ranking depending on dataset characteristics and prediction targets.

This consistent hierarchy reflects the fundamental strengths of ensemble methods: XGBoost's gradient-boosting framework excels at capturing complex nonlinear interactions while maintaining resistance to overfitting through regularization; GPR provides probabilistic outputs with excellent uncertainty quantification; Random Forest offers superior interpretability at modest accuracy trade-offs. The practical implication is that algorithm selection should be guided by application requirements: regulatory-sensitive decisions (e.g., site selection, risk assessment) favor interpretable RF models, while high-accuracy predictions for operational optimization favor XGBoost or GPR.

6.1.2. The Critical Role of Field-Scale Validation

A second emergent theme is the critical importance of field-scale validation for ML model credibility and practical adoption. Studies that validated ML models on real field data consistently demonstrated lower R^2 values compared to synthetic validations, reflecting the inherent complexity and heterogeneity of real-world reservoirs. For example, Vo Thanh and Lee [15] achieved R^2 = 0.999 on synthetic test data but R^2 = 0.9935 when validated on field data from the Cuu Long Basin, a modest but meaningful reduction. Similarly, Abdulkhaleq et al. [56] achieved R^2 values of 0.962, 0.847, and 0.849 for different objectives on the Tensleep formation, highlighting the gap between laboratory/synthetic accuracy and field performance.

This pattern underscores that ML models trained on synthetic or idealized datasets may exhibit "accuracy inflation" that does not translate to field deployment. The implication is that rigorous field validation, even with reduced accuracy metrics, is essential for building trust in ML predictions for CCS applications.

6.1.3. The Convergence of Monitoring and ML Technologies

A third emergent theme is the convergence of advanced monitoring technologies with ML analytics. The integration of 4D seismic data [37,95], distributed fiber-optic sensing (DTS/DAS) [35], and real-time pressure monitoring [66,67] with ML algorithms is enabling unprecedented levels of subsurface surveillance. The cost-sensitivity analysis (Figure 6) reveals that optimal monitoring strategies combine multiple techniques—high-sensitivity methods (crosswell tomography, downhole logging) for detailed characterization paired with continuous techniques (pressure monitoring, atmospheric sensing) for ongoing surveillance.

6.1.4. The Imperative of Geological Uncertainty Consideration

Robust optimization under geological uncertainty has been shown to improve CO_2 trapping by 15–28% compared to nominal optimization [17]. This finding, validated

across multiple reservoir types and injection scenarios, demonstrates that accounting for geological uncertainty is not merely an academic exercise but a practical necessity for maximizing storage efficiency and reducing project risks. The implication is that uncertainty quantification should be standard practice in CCS project design rather than an optional enhancement.

6.2. Comparison of Conflicting Results and Explanation of Discrepancies

While many findings are consistent across studies, several apparent conflicts emerge in the reviewed literature that warrants careful examination.

6.2.1. XGBoost vs. GPR vs. RF: Which Algorithm Is "Best"?

The reviewed studies present seemingly conflicting performance rankings. Vo Thanh et al. [15] ranked XGBoost highest (R^2 = 0.9993), while Safaei-Farouji et al. [55] ranked RF highest (R^2 = 0.995), and Vo Thanh and Lee [15] ranked GPR highest (R^2 = 0.992). However, these discrepancies are explained by differences in dataset characteristics and prediction targets:

Dataset size and diversity: XGBoost excels with larger, more diverse datasets (1509 samples from 33 fields) where its regularization prevents overfitting [15]. RF performs well with moderate datasets (1868 samples) where its ensemble nature provides robustness [55]. GPR shows particular strength with smaller datasets where its probabilistic framework provides meaningful uncertainty quantification [15].

Prediction target: XGBoost demonstrates particular strength for solubility trapping (R^2 = 0.9993), while RF shows comparable performance for residual trapping (R^2 = 0.995). GPR excels when uncertainty quantification is prioritized over point prediction accuracy.

Interpretability requirements: RF offers superior interpretability through feature importance analysis, making it preferred for regulatory-sensitive applications despite slightly lower accuracy.

The practical implication is that no single algorithm is universally "best"; rather, algorithm selection should be guided by dataset characteristics, prediction targets, and application requirements.

6.2.2. Deep Learning Speedup vs. Accuracy Trade-Off

Yan et al. [36] reported that FNO-based deep learning surrogates achieved 250× speedup compared to full physics simulation while maintaining high predictive fidelity. However, this speedup comes with trade-offs: the deep learning models are "black boxes" with limited interpretability, require extensive training data, and may extrapolate poorly outside their training domain. In contrast, simpler surrogate models (e.g., MARS, RF) offer greater interpretability and easier deployment at the cost of reduced speedup (typically 10–100×). The choice between these approaches depends on the specific application: real-time operational optimization may justify the speed-accuracy trade-off, while regulatory submissions may require the interpretability of simpler models.

6.2.3. Monitoring Technique Effectiveness

The reviewed literature presents apparently conflicting assessments of monitoring technique effectiveness. Chen et al. [19] found that pressure data provide higher value of information than CO_2 saturation or temperature data. However, Sambo et al. [95] ranked 4D seismic as most reliable for imaging CO_2 distribution. These findings are not contradictory but reflect different evaluation criteria: pressure data excel for continuous, real-time surveillance, while 4D seismic excels for detailed spatial characterization. The optimal monitoring strategy combines both pressure monitoring for continuous surveillance and periodic seismic surveys for detailed plume imaging.

6.2.4. The Role of Cement Degradation in CCS Risk

Alsubaih et al. [35] demonstrated that self-healing cement formulations maintain porosity increases below 4% under CO_2 exposure, while conventional cement degrades by over 17%. However, some studies suggest that cement degradation may be less critical than other risk factors (e.g., fault reactivation, legacy wells). These perspectives are not contradictory but reflect different risk assessment timeframes: cement degradation is a long-term risk (decades to centuries), while fault reactivation and legacy well leakage present more immediate operational risks. The implication is that risk mitigation strategies must address both short-term operational risks and long-term material degradation.

6.3. Critical Evaluation of Limitations of Reviewed Methods

Despite significant advances, the reviewed ML methods and CCS applications exhibit several important limitations that must be acknowledged.

6.3.1. Data Limitations

Synthetic data dominance: A majority of ML studies in CCS are trained on synthetic or laboratory-generated datasets. While such studies provide valuable proof-of-concept and methodological development, they may not capture the full complexity of heterogeneous, real-world reservoirs. The performance gap between synthetic validation ($R^2 > 0.99$) and field validation ($R^2 \approx 0.85$–0.95) documented in multiple studies underscores this limitation [15,56].

Data scarcity: Subsurface data are inherently expensive to acquire, resulting in limited sample sizes for ML training. While studies with 1500–6800 samples [15,55,143] represent progress, they remain small compared to typical ML benchmarks. This scarcity limits the application of data-hungry deep learning methods and necessitates careful feature engineering and regularization.

Data heterogeneity: The reviewed studies use diverse datasets with varying geological settings, injection conditions, and measurement protocols. While heterogeneity enhances model generalizability, it also complicates direct comparison of results across studies and may obscure important site-specific effects.

6.3.2. Model Interpretability

The "black box" nature of deep learning models and complex ensemble methods (e.g., XGBoost, GPR) poses significant challenges for regulatory acceptance and operational trust in safety-critical CCS applications. While SHAP, LIME, and other explainable AI techniques provide partial interpretability [16], they do not fully address the need for physically transparent and verifiable predictions. The trade-off between accuracy and interpretability (Figure 4) is a fundamental challenge that requires explicit consideration in algorithm selection.

6.3.3. Generalization and Extrapolation

ML models are fundamentally interpolation tools and may fail when extrapolating beyond their training domain. This limitation is particularly acute for CCS applications where novel reservoir conditions, injection strategies, or operational scenarios may fall outside the training data distribution. Surrogate models trained on limited simulation scenarios may produce inaccurate predictions for conditions not represented in the training dataset—a risk that is often underappreciated in ML-based CCS studies.

6.3.4. Computational Constraints

While ML surrogates dramatically reduce simulation time (250× speedup reported by Yan et al. [36]), training deep learning models requires substantial computational resources

and expertise. The training time for FNO-based surrogates (2.25 h on GPU) and the need for large training datasets (90 simulation runs) may be prohibitive for some CCS applications, particularly in resource-constrained settings.

6.3.5. Integration Challenges

ML models are often developed in isolation from operational workflows, leading to integration challenges in real-world CCS projects. The absence of standardized interfaces, data formats, and validation protocols complicates the deployment of ML tools in operational settings. Legacy CCS infrastructure and conservative industry culture further slow adoption.

6.3.6. ML vs. Physical Modeling: When Does ML Surpass and When Does It Fit Noise?

A critical question underlying any ML application in CCS is whether ML genuinely advances predictive capability beyond physical modeling, or whether it merely fits noise on limited datasets. This distinction is essential for responsible deployment and regulatory acceptance.

Machine learning genuinely surpasses physical modeling in several well-defined scenarios. First, ML excels at high-dimensional pattern recognition, detecting complex, nonlinear relationships that are difficult to capture with physics-based models. This is evidenced by studies achieving $R^2 = 0.9993$ for CO_2 trapping prediction from 1509 field samples using XGBoost [15]. Second, ML provides dramatic computational acceleration, with Fourier Neural Operator-based surrogates reducing simulation time by factors of 250 or more while maintaining high predictive fidelity [37]. Third, ML enables effective data fusion, integrating heterogeneous data types, seismic, well logs, pressure, and production data, for applications such as history matching with 4D seismic and monitoring well data [144]. Fourth, ML supports real-time decision support, providing predictions in milliseconds versus hours or days for conventional simulators, as demonstrated in smart injection control systems [16]. Fifth, ML excels at anomaly detection, identifying subtle patterns in high-frequency sensor data using architectures such as ConvLSTM and CNN-BiLSTM for pressure anomaly detection [66,67].

Conversely, ML risks fitting noise under several conditions. When datasets are small, ML models tend to overfit to spurious correlations, necessitating the use of simpler models such as Random Forest or Support Vector Regression with regularization, or Gaussian Process Regression for uncertainty quantification. When models are trained predominantly on synthetic data, they may learn artificial patterns that do not generalize to real-world conditions, a problem that can be mitigated by requiring field validation and reporting the accuracy gap between synthetic and field performance. When extrapolation beyond the training domain is required, ML models often fail because conditions differ from those represented in the training data; this risk can be managed by restricting predictions to the training domain, using physics-informed ML approaches, or validating against physical models. When models lack physical constraints, they may violate conservation laws; integrating mass balance, thermodynamic principles, and geomechanical constraints into ML architectures addresses this limitation. Finally, when black-box predictions are used for safety-critical decisions, the lack of interpretability undermines trust, favoring the use of interpretable models such as Random Forest or explainable AI techniques such as SHAP and LIME.

For practitioners, this framework provides clear guidance. ML is preferable when large, high-quality field datasets are available (>1000 samples), when relationships are complex and nonlinear, when computational speed is critical for real-time decisions, when multiple data types must be integrated, or when the task involves pattern recognition such

as anomaly detection or image interpretation. Physical modeling is preferable when data are scarce (<200 samples), when physical understanding is strong and well-validated, when extrapolation beyond known conditions is required, when regulatory submissions require physically based predictions, or when the task involves well-understood linear or weakly nonlinear physics. Hybrid approaches that combine ML with physical constraints are preferable when moderate data are available (200–1000 samples), when physical constraints must be enforced, when both speed and accuracy are required, when uncertainty quantification is critical, or when the application involves coupled physical processes such as thermo-hydro-mechanical-chemical (THMC) effects. This framework enables practitioners to make informed decisions about when ML is genuinely valuable versus when it may introduce unwarranted complexity or risk.

6.4. Open Knowledge Gaps and Future Research Priorities

Despite the substantial progress documented in this review, several critical knowledge gaps remain that require focused research attention.

6.4.1. Physics-Informed ML Integration

While hybrid ML-physics approaches show promise [37,81], they remain underdeveloped relative to purely data-driven methods. Future research should prioritize the integration of physical constraints (mass conservation, thermodynamic laws, geomechanical principles) into ML architectures to enhance physical consistency, improve extrapolation capability, and increase regulatory acceptance. Physics-informed neural networks (PINNs) and constraint-encoded ensemble methods represent promising directions.

Future research should prioritize the integration of physical constraints into ML architectures. Physics-Informed Neural Networks (PINNs) represent a particularly promising direction, as they embed governing physical laws directly into the loss function, ensuring consistency with conservation principles. For CCS, PINNs could be applied to enforce mass balance in plume predictions, constrain geomechanical simulations, and enable reliable extrapolation beyond training data. However, challenges include computational cost for large-scale problems, the need for accurate physical parameterization, and integration with existing simulation workflows. Hybrid approaches that combine PINNs with data-driven ensemble methods may offer the optimal balance of physical consistency and predictive accuracy.

6.4.2. Standardized Benchmarking and Validation

The field lacks standardized benchmark datasets and evaluation protocols for ML in CCS applications. This absence complicates fair comparison of methods, hinders scientific progress, and limits regulatory acceptance. Future work should develop:

- Open-source benchmark datasets representing diverse geological settings and operational conditions
- Standardized evaluation metrics and validation protocols
- Reproducible ML pipelines for CCS applications

6.4.3. Uncertainty Quantification

While GPR and ensemble methods provide some uncertainty estimates, comprehensive uncertainty quantification for ML predictions in CCS remains underdeveloped. Future research should focus on:

- Bayesian deep learning for CCS applications
- Ensemble-based uncertainty quantification
- Confidence calibration for ML predictions

- Integration of uncertainty estimates into operational decision-making

6.4.4. Long-Term Performance Prediction

CCS projects require performance predictions over decadal to centennial timeframes, while most ML models are trained on relatively short-term data. The extrapolation of ML predictions to long-term performance remains a critical gap. Research should address:

- Transfer learning from short-term to long-term predictions
- Integration of mechanistic degradation models with ML
- Validation against long-term field data (e.g., Sleipner's 20+ years of operation)

6.4.5. Digital Twin Integration

While digital twin technology shows promise for CCS applications [35], its integration with ML-based predictive models remains nascent. Future research should address:

- Real-time data assimilation for digital twins
- ML-enhanced model updating and calibration
- Predictive maintenance and remaining useful life (RUL) estimation
- Autonomous control and optimization frameworks

6.4.6. Regulatory Frameworks for ML-Assisted CCS

The absence of regulatory frameworks for ML-assisted CCS decisions represents a significant barrier to adoption. Research is needed to:

- Develop guidelines for ML model validation and verification
- Establish standards for explainability and transparency
- Create frameworks for uncertainty communication to regulators and stakeholders

6.4.7. Legacy Well Risk Assessment

The presence of millions of orphaned and abandoned wells [125] poses a critical challenge for CCS deployment. While Alsubaih et al. [125] demonstrated ML-based prediction of orphan well locations; comprehensive risk assessment frameworks that integrate ML predictions with operational decision-making remain underdeveloped. Future research should address:

- Probabilistic risk assessment for legacy well leakage
- Integration of well integrity data with reservoir simulation
- Prioritization of remediation efforts based on ML-based risk scoring

6.4.8. Cost-Effective Monitoring Optimization

While the cost-sensitivity analysis (Figure 6) provides qualitative guidance for monitoring strategy selection, quantitative optimization of monitoring networks remains an open challenge. Future research should develop:

- ML-based optimization of sensor placement and monitoring frequency
- Value of information (VOI) frameworks for monitoring design
- Integration of monitoring costs with risk reduction benefits

6.5. Summary of Discussion

This discussion has synthesized the reviewed evidence across four themes, compared conflicting results and explained their underlying discrepancies, critically evaluated the limitations of reviewed methods, and identified open knowledge gaps with prioritized research directions. The analysis reveals that while ML has demonstrated transformative potential across the CCS lifecycle, realizing this potential requires addressing fundamen-

tal challenges in data availability, model interpretability, generalization, computational constraints, and integration with operational workflows. The prioritized research agenda, encompassing physics-informed ML, standardized benchmarking, uncertainty quantification, long-term prediction, digital twin integration, regulatory frameworks, legacy well risk assessment, and cost-effective monitoring, provides a roadmap for advancing the field and accelerating the deployment of ML-assisted CCS.

7. Conclusions

This review has systematically examined the integration of machine learning across the carbon capture and storage lifecycle, encompassing pre-injection evaluation, injection optimization, and post-injection monitoring. The analysis reveals that ML has matured from a promising research tool to a practical technology with demonstrated value across multiple CCS applications. This section synthesizes the key findings, articulates the practical and policy implications, and outlines a forward-looking agenda for realizing the full potential of ML-assisted CCS.

7.1. Summary of Key Findings

The reviewed evidence establishes several robust findings that transcend individual studies and methodological approaches:

Algorithm Performance Hierarchy: XGBoost and Gaussian Process Regression consistently achieve the highest predictive accuracy ($R^2 > 0.99$) for CO_2 trapping efficiency, while Random Forest offers competitive performance ($R^2 \approx 0.95$–0.98) with superior interpretability. The choice between these algorithms should be guided by the specific application: regulatory-sensitive decisions favor interpretable models, while high-accuracy operational optimization favors boosting methods.

Computational Acceleration: Deep learning surrogates, particularly Fourier Neural Operators, can accelerate plume simulations by factors of 250 or more compared to full physics simulation, making previously intractable problems, such as rigorous uncertainty quantification for large-scale storage projects, computationally feasible.

Uncertainty Matters: Robust optimization under geological uncertainty improves CO_2 trapping by 15–28% compared to nominal optimization, demonstrating that accounting for geological heterogeneity is not merely an academic exercise but a practical necessity for maximizing storage efficiency.

Monitoring Convergence: The integration of ML with advanced monitoring technologies (4D seismic, distributed fiber-optic sensing, real-time pressure monitoring) enables unprecedented subsurface surveillance. The optimal monitoring strategy combines high-sensitivity techniques for detailed characterization with continuous techniques for ongoing surveillance.

Wellbore Integrity Critical: Coupled thermo-hydro-chemo-mechanical effects critically control long-term storage security. Self-healing cement formulations maintain porosity increases below 4%, whereas conventional cement degrades by over 17% under CO_2 exposure. Smart injection systems using reinforcement learning reduce CO_2 leakage through legacy wells by up to 84%.

Legacy Well Risk: Over 225,000 documented orphaned wells in the United States, with millions more undocumented—pose a significant challenge for CCS site selection, necessitating ML-based prediction tools for risk screening and remediation prioritization.

7.2. Practical Implications for CCS Operations

The findings of this review have several practical implications for CCS operators and project developers:

Algorithm Selection Protocol: Operators should adopt a structured approach to algorithm selection based on application requirements. For site screening and regulatory submissions, Random Forest's interpretability is advantageous. For operational optimization where prediction accuracy is paramount, XGBoost or GPR should be preferred. For uncertainty quantification, GPR's probabilistic framework provides unique value.

Monitoring Network Design: The cost-sensitivity analysis (Figure 6) provides a framework for designing cost-effective monitoring networks. Operators should combine pressure monitoring (low cost, continuous) for routine surveillance with periodic 4D seismic surveys (high cost, high resolution) for detailed plume imaging. The incremental benefit of additional monitoring wells diminishes beyond a certain threshold.

Injection Strategy Optimization: Robust optimization under geological uncertainty should be standard practice rather than an optional enhancement. The 15–28% improvement in CO_2 trapping documented in this review justifies the additional computational investment.

Legacy Well Risk Management: CCS projects must conduct rigorous legacy well screening and, where necessary, re-abandonment campaigns before operations can safely commence. ML-based prediction of undocumented orphan wells can inform risk-based prioritization of remediation efforts.

Wellbore Integrity Investment: Long-term storage security depends critically on wellbore integrity. Investment in self-healing cement formulations and smart injection systems should be prioritized for CCS projects, as they provide demonstrable improvements in leakage prevention.

7.3. Policy Implications and Recommendations

The findings of this review have significant implications for policymakers, regulators, and international bodies working to enable large-scale CCS deployment.

7.3.1. Regulatory Frameworks for ML-Assisted CCS

Current regulatory frameworks do not adequately address the use of ML for CCS decision-making. Regulators should carry out the following:

- Develop validation standards for ML models used in safety-critical CCS applications, including requirements for model transparency, uncertainty quantification, and field validation.
- Establish guidelines for explainability, requiring that ML predictions used for regulatory submissions be accompanied by interpretability analysis (e.g., SHAP, feature importance) that enables human oversight.
- Create frameworks for uncertainty communication, ensuring that ML prediction uncertainties are appropriately conveyed to regulators, stakeholders, and the public.
- Enable iterative model updating, allowing ML models to be refined as new monitoring data become available, improving prediction accuracy over time.

7.3.2. Standardization and Data Sharing

The absence of standardized benchmark datasets and evaluation protocols hinders scientific progress and regulatory acceptance. Policymakers should carry out the following:

- Support the development of open-source benchmark datasets for CCS ML applications, representing diverse geological settings and operational conditions.
- Encourage data sharing among CCS projects, operators, and research institutions to build larger, more diverse training datasets that enhance model generalizability.
- Promote the adoption of standardized evaluation metrics and validation protocols to enable fair comparison of ML methods.

- Support the development of reproducible ML pipelines that facilitate technology transfer from research to operational deployment.

7.3.3. Investment and Incentive Structures

The economic viability of CCS projects can be enhanced through ML-enabled cost reduction. Policymakers should carry out the following:

- Incentivize ML adoption through tax credits, grants, or favorable regulatory treatment for projects that demonstrate robust ML-based risk management.
- Support research and development in priority areas identified in this review, including physics-informed ML, uncertainty quantification, and digital twin integration.
- Fund field validation studies that bridge the gap between laboratory/synthetic ML development and operational deployment.
- Create public–private partnerships to accelerate the development and deployment of ML tools for CCS.

7.3.4. International Collaboration

CCS deployment requires international coordination to achieve climate goals. Policymakers should carry out the following:

- Promote international standards for ML-assisted CCS, ensuring consistency across jurisdictions.
- Facilitate knowledge transfer between regions with advanced CCS capabilities (e.g., Europe, North America) and regions with emerging CCS programs.
- Support collaborative research on cross-cutting challenges such as legacy well risk assessment and long-term monitoring.
- Align ML development with climate policy goals, ensuring that ML-assisted CCS contributes to net-zero emission targets.

7.3.5. Workforce Development

The interdisciplinary nature of ML-assisted CCS requires new skills and expertise. Policymakers and industry should carry out the following:

- Invest in education and training at the intersection of data science, geoscience, and petroleum engineering.
- Support interdisciplinary research programs that bring together ML researchers, geoscientists, and engineers.
- Encourage industry-academia collaboration to ensure that ML research addresses real-world CCS challenges.
- Develop certification programs for ML practitioners in CCS applications.

7.4. Open Challenges and Future Research Priorities

Despite the substantial progress documented in this review, several critical challenges remain that require focused research attention:

- Physics-Informed ML: The integration of physical constraints (mass conservation, thermodynamic laws, geomechanical principles) into ML architectures remains underdeveloped. Future research should prioritize physics-informed neural networks and constraint-encoded ensemble methods to enhance physical consistency and regulatory acceptance.
- Standardized Benchmarking: The field lacks standardized benchmark datasets and evaluation protocols for ML in CCS applications. Future work should develop open-source benchmarks, standardized metrics, and reproducible pipelines.

- Uncertainty Quantification: Comprehensive uncertainty quantification for ML predictions remains underdeveloped. Research should focus on Bayesian deep learning, ensemble-based methods, and confidence calibration for CCS applications.
- Long-Term Performance Prediction: CCS projects require performance predictions over decadal to centennial timeframes. Research should address transfer learning from short-term to long-term predictions and integration of mechanistic degradation models with ML.
- Digital Twin Integration: While digital twin technology shows promise, its integration with ML-based predictive models remains nascent. Research should address real-time data assimilation, predictive maintenance, and autonomous control frameworks.
- Legacy Well Risk Assessment: Comprehensive risk assessment frameworks that integrate ML predictions with operational decision-making for legacy well leakage remain underdeveloped.

7.5. Concluding Remarks

Machine learning has demonstrated transformative potential across the CCS lifecycle, from pre-injection site selection to post-injection monitoring. The evidence reviewed in this paper establishes that ML can accelerate simulations by factors of 250 or more, improve prediction accuracy to $R^2 > 0.99$, reduce CO_2 leakage by up to 84%, and optimize injection strategies to improve trapping by 15–28%. These capabilities translate directly to reduced costs, enhanced safety, and improved storage security.

However, realizing the full potential of ML-assisted CCS requires addressing fundamental challenges in data availability, model interpretability, generalization, and integration with operational workflows. The prioritized research agenda, encompassing physics-informed ML, standardized benchmarking, uncertainty quantification, long-term prediction, digital twin integration, regulatory frameworks, and legacy well risk assessment, provides a roadmap for advancing the field.

Policy action is urgently needed to establish regulatory frameworks for ML-assisted CCS, promote standardization and data sharing, create incentive structures for ML adoption, and support the interdisciplinary workforce development required for this emerging field. International collaboration will be essential to accelerate progress and ensure that ML contributes effectively to global net-zero emission targets.

Ultimately, the integration of ML into CCS represents not merely a technical enhancement but a paradigm shift in how we approach subsurface storage. By enabling data-driven decision-making, reducing uncertainty, and improving operational efficiency, ML can help unlock the full potential of geological carbon sequestration as a cornerstone of climate change mitigation.

7.6. A Unified ML Framework for CCS: Implementation Blueprint

While this review has synthesized ML applications across the CCS lifecycle, a critical gap remains between research advances and operational deployment. To bridge this gap, we propose a unified ML framework that provides a structured pipeline for implementing ML in CCS projects. The framework consists of five interconnected modules, as illustrated in Figure 9.

The outlined five modules in Figure 9 are illustrated, and they are as follows:

Module 1: Data Layer. The foundation of any ML application is the data layer, which encompasses all relevant data sources for CCS operations. This includes geological data (porosity, permeability, structure, lithology), well logs (gamma ray, resistivity, density, sonic), seismic data (2D/3D/4D attributes), production and injection data (rates, pressures, temperatures), monitoring data (pressure, temperature, seismic, geochemical), and litera-

ture or field data from published studies. For CCS applications, special consideration must be given to the heterogeneous nature of subsurface data, the sparse well coverage typical of many reservoirs, the temporal resolution of monitoring data, and the quality control required for field measurements. The data layer must also address uncertainty quantification in geological properties, which is essential for robust ML model development.

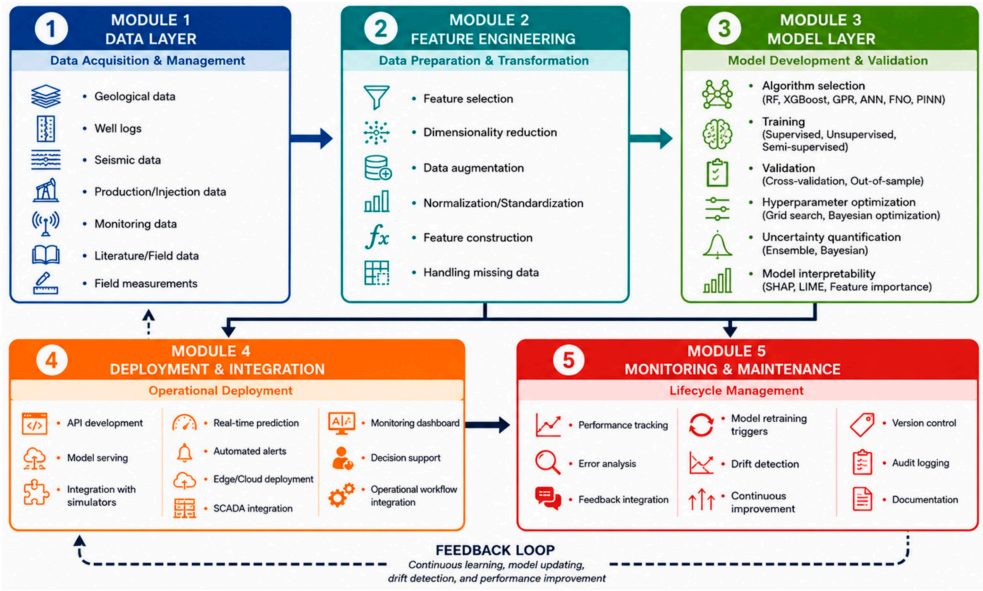

Figure 9. Unified ML framework for CCS—implementation blueprint.

Module 2: Feature Engineering. The feature engineering module transforms raw data into meaningful input variables for ML models. This involves feature selection to identify the most relevant geological, petrophysical, and operational parameters; dimensionality reduction using techniques such as Principal Component Analysis (PCA) or autoencoders to manage high-dimensional data; and data augmentation through synthetic data generation or transfer learning to address data scarcity. Normalization and scaling are essential for handling different physical units across variables. Feature construction, creating derived features such as ratios, gradients, or physics-based combinations, incorporates domain knowledge directly into the ML pipeline. Missing data handling through imputation or uncertainty propagation is particularly critical for CCS applications where well logs and monitoring data may have gaps or inconsistent coverage.

Module 3: Model Layer. The model layer encompasses algorithm selection, training, validation, hyperparameter optimization, uncertainty quantification, and interpretability analysis. Algorithm selection should be guided by the specific application: Random Forest for regulatory-sensitive decisions requiring interpretability; XGBoost or GPR for high-accuracy predictions; deep learning architectures (FNO, CNN, LSTM) for large-scale spatial-temporal problems; and Physics-Informed Neural Networks (PINNs) when physical constraints must be enforced. Training must employ appropriate validation strategies, including cross-validation and out-of-sample testing with geological grouping to avoid data leakage. Hyperparameter optimization using grid search or Bayesian methods prevents overfitting. Uncertainty quantification through ensemble methods or Bayesian approaches provides confidence intervals essential for risk assessment. Interpretability analysis using SHAP, LIME, or feature importance ensures regulatory acceptance and operator trust.

Module 4: Deployment and Integration. The deployment module translates ML models from research to operational use. This involves developing APIs (REST APIs) for model access and integration with existing operational systems; implementing real-time prediction capabilities with millisecond inference times to meet operational constraints;

establishing automated alerting systems based on rule-based or ML-triggered events with careful false positive management; integrating ML models with existing simulators for surrogate model use and hybrid approaches; connecting to SCADA systems for operational data pipelines; and developing decision support tools with clear visualizations and actionable recommendations for engineers. This module requires close collaboration between data scientists, reservoir engineers, and IT specialists to ensure seamless integration.

Module 5: Monitoring and Maintenance. The final module ensures that ML models remain accurate and reliable over time. This includes performance tracking to monitor prediction accuracy over time and detect bias or drift as reservoir conditions change; automated or scheduled model retraining triggered by new data availability or performance degradation; drift detection for both data drift (changes in input distributions) and concept drift (changes in underlying relationships); version control for models and data to ensure reproducibility and audit trails; and audit logging of prediction records and decisions for regulatory compliance. For CCS applications, where reservoir conditions evolve over decades, this module is particularly critical for maintaining prediction reliability throughout the injection and post-injection monitoring periods.

Implementation Roadmap for Practitioners. The framework can be implemented in four phases. Phase 1—Assessment (0–3 months) involves defining the problem and success criteria, auditing available data quality and quantity, identifying gaps and prioritizing data collection, and selecting the appropriate ML approach based on data availability and application context. Phase 2—Development (3–6 months) includes data preparation and feature engineering, model training and validation, hyperparameter optimization, uncertainty quantification, and interpretability analysis. Phase 3—Integration (6–9 months) focuses on building APIs for model serving, integrating with operational workflows, developing monitoring dashboards, and establishing alerting mechanisms. Phase 4—Deployment and Maintenance (ongoing) involves deploying in pilot operations, monitoring performance and retraining as needed, documenting lessons learned, and scaling to full operations.

Cost–Benefit Considerations. The value of ML implementation varies with data availability and application context. For data-scarce environments (<200 samples), physical modeling with simple ML (RF, SVR) is recommended, with expected accuracy improvements of 5–15% and low to medium development effort. For data-moderate environments (200–1000 samples), hybrid approaches combining PINNs with GPR are appropriate, offering 10–25% accuracy improvements with medium development and maintenance effort. For data-rich environments (>1000 samples), full ML implementation with XGBoost or deep learning is feasible, providing 20–40% accuracy improvements but requiring higher development and maintenance effort. Regulatory acceptance varies inversely with model complexity: physics-based approaches enjoy high acceptance, hybrid approaches medium acceptance, and black-box models low acceptance unless accompanied by robust interpretability and validation.

This framework provides engineers with a practical, modular blueprint for implementing ML in CCS projects, from data acquisition to operational deployment, while addressing the critical gaps identified in this review.

Author Contributions: Conceptualization, W.J.A.-M., A.A. and K.S.; methodology, W.J.A.-M., A.A. and K.S.; validation, W.J.A.-M. and A.A.; formal analysis, W.J.A.-M. and K.S.; investigation, W.J.A.-M. and K.S.; resources, W.J.A.-M., A.A. and K.S.; data curation, A.A.; writing—original draft preparation, W.J.A.-M. and A.A.; writing—review and editing, W.J.A.-M., A.A. and K.S.; visualization, W.J.A.-M.; supervision, K.S.; project administration, W.J.A.-M. All authors have read and agreed to the published version of the manuscript.

Funding: This research received no external funding.

Data Availability Statement: The original contributions presented in the study are included in the article, further inquiries can be directed to the corresponding author.

Acknowledgments: During the preparation of this work, the author used DeepSeek-V4 to generate some paragraphs. After using this tool, the author reviewed and edited the content as needed and took full responsibility for the content of the publication.

Conflicts of Interest: Author Watheq J. Al-Mudhafar was employed by the company Basrah Oil Company. The remaining authors declare that the research was conducted in the absence of any commercial or financial relationships that could be construed as a potential conflict of interest.

Nomenclature

Abbreviation	Definition
General CCS Terms	
AI	Artificial Intelligence
ANN	Artificial Neural Network
CCS	Carbon Capture and Storage
CCUS	Carbon Capture, Utilization, and Storage
CNN	Convolutional Neural Network
CPU	Central Processing Unit
DL	Deep Learning
EOR	Enhanced Oil Recovery
FNO	Fourier Neural Operator
GCS	Geological Carbon Sequestration
GHG	Greenhouse Gas
GNN	Graph Neural Network
GPU	Graphics Processing Unit
GPR	Gaussian Process Regression
LHS	Latin Hypercube Sampling
LSTM	Long Short-Term Memory
MAE	Mean Absolute Error
MARS	Multivariate Adaptive Regression Splines
MCMC	Markov Chain Monte Carlo
ML	Machine Learning
MLP	Multilayer Perceptron
MSE	Mean Square Error
MVA	Monitoring, Verification, and Accounting
OOB	Out-of-Bag
PCA	Principal Component Analysis
PINN	Physics-Informed Neural Network
PSO	Particle Swarm Optimization
RBF	Radial Basis Function
RBFNN	Radial Basis Function Neural Network
ReLU	Rectified Linear Unit
RF	Random Forest
RMSE	Root Mean Square Error
ROC	Receiver Operating Characteristic
ROM	Reduced-Order Model
RNN	Recurrent Neural Network
SVR	Support Vector Regression
WAG	Water-Alternating Gas
XGBoost	Extreme Gradient Boosting

Geological and Reservoir Terms	
AZMI	Above Zone Monitoring Intervals
BHP	Bottom Hole Pressure
CART	Classification and Regression Tree
FEHM	Finite Element Heat and Mass Transfer
kv/kh	Vertical-to-Horizontal Permeability Ratio
RTI	Residual Trapping Index
STI	Solubility Trapping Index
TEI	Total Efficiency Index
TTI	Total Trapping Index
UCS	Unconfined Compressive Strength
Optimization and Statistical Terms	
ABC	Artificial Bee Colony
ANFIS	Adaptive Neuro-Fuzzy Inference System
AO	Aquila Optimizer
AOSSA	Aquila Optimizer-Salp Swarm Algorithm
DECE	Design Exploration and Controlled Evolution
ET	Extra Tree
GA	Genetic Algorithm
LHS	Latin Hypercube Design
MFO	Moth-Flame Optimization
MVO	Multi-Verse Optimization
RSM	Response Surface Methodology
SCA	Sine-Cosine Algorithm
SSA	Salp Swarm Algorithm
SHAP	SHapley Additive exPlanations
LIME	Local Interpretable Model-agnostic Explanations
VOI	Value of Information
RUL	Remaining Useful Life
Monitoring and Field Terms	
4D	Four-Dimensional (Time-Lapse)
FWI	Full-Waveform Inversion
IBDP	Illinois Basin-Decatur Project
InSAR	Interferometric Synthetic Aperture Radar
IRMDSS	Integrated Risk Management and Decision Support System
LI	Leakage Index
NRAP	National Risk Assessment Partnership
PV	Pore Volume
TDS	Total Dissolved Solids

References

1. Benson, S.M.; Cole, D.R. CO_2 sequestration in deep sedimentary formations. *Elements* **2008**, *4*, 325–331. [CrossRef]
2. Baz, H.; Noureldin, M.; Allinson, W.G.; Cinar, Y. A field-scale investigation of residual and dissolution trapping of CO_2 in a saline formation in Western Australia. *Int. J. Greenh. Gas Control* **2016**, *46*, 86–99. [CrossRef]
3. Soltanian, M.R.; Amooie, M.A.; Cole, D.R.; Graham, D.E.; Hosseini, S.A.; Hovorka, S.; Pfiffner, S.M.; Phelps, T.J.; Moortgat, J. Simulating the Cranfield geological carbon sequestration project with high-resolution static models and an accurate equation of state. *Int. J. Greenh. Gas Control* **2016**, *54*, 282–296. [CrossRef]
4. Sohal, M.A.; Le Gallo, Y.; Audigane, P.; de Dios, J.C.; Rigby, S.P. Effect of geological heterogeneities on reservoir storage capacity and migration of CO_2 plume in a deep saline fractured carbonate aquifer. *Int. J. Greenh. Gas Control* **2021**, *108*, 103306. [CrossRef]
5. Singh, M.; Chaudhuri, A.; Soltanian, M.R.; Stauffer, P.H. Coupled multiphase flow and transport simulation to model CO_2 dissolution and local capillary trapping in permeability and capillary heterogeneous reservoir. *Int. J. Greenh. Gas Control* **2021**, *108*, 103329. [CrossRef]
6. Dejam, M.; Hassanzadeh, H. Diffusive leakage of brine from aquifers during CO_2 geological storage. *Adv. Water Resour.* **2018**, *111*, 36–57. [CrossRef]

7. Szulczewski, M.L.; MacMinn, C.W.; Herzog, H.J.; Juanes, R. Lifetime of carbon capture and storage as a climate-change mitigation technology. *Proc. Natl. Acad. Sci. USA* **2012**, *109*, 5185–5189. [CrossRef] [PubMed]
8. Nghiem, L.; Yang, C.; Shrivatava, V.; Kohse, B.; Hassam, M.; Chen, D.; Card, C. Optimization of residual gas and solubility trapping for CO_2 storage in saline aquifers. *Energy Procedia* **2009**, *1*, 1–9. [CrossRef]
9. Menad, N.A.; Hemmati-Sarapardeh, A.; Varamesh, A.; Shamshirband, S. Predicting solubility of CO_2 in brine by advanced machine learning systems: Application to carbon capture and sequestration. *J. CO_2 Util.* **2019**, *33*, 83–95. [CrossRef]
10. Mahdaviara, M.; Nait, M.; Hemmati-Sarapardeh, A. Toward smart schemes for modeling CO_2 solubility in crude oil: Application to carbon dioxide enhanced oil recovery. *Fuel* **2021**, *285*, 119147. [CrossRef]
11. Al-Mudhafar, W.J. Polynomial and nonparametric regressions for efficient predictive proxy metamodeling: Application through the CO_2-EOR in shale oil reservoirs. *J. Nat. Gas Sci. Eng.* **2019**, *72*, 103038. [CrossRef]
12. Jeong, H.; Sun, A.Y.; Lee, J.; Min, B. A learning-based data-driven forecast approach for predicting future reservoir performance. *Adv. Water Resour.* **2018**, *118*, 95–109. [CrossRef]
13. Ganesh, P.R.; Mishra, S. Simplified physics model of CO_2 plume extent in stratified aquifer-caprock systems. *Greenh. Gases Sci. Technol.* **2016**, *6*, 70–82. [CrossRef]
14. Zhang, J.; Feng, Q.; Zhang, X.; Shu, C.; Wang, S.; Wu, K. A supervised learning approach for accurate modeling of CO_2–brine interfacial tension with application in identifying the optimum sequestration depth in saline aquifers. *Energy Fuels* **2020**, *34*, 7353–7362. [CrossRef]
15. Vo Thanh, H.; Lee, K.-K. Application of machine learning to predict CO_2 trapping performance in deep saline aquifers. *Energy* **2022**, *239*, 122457. [CrossRef]
16. Alsubaih, A.; Femande, B.; Delshad, M.; Sepehrnoori, K. Comparative evaluation of brine leakage models in legacy wells: Analytical, transient, and mechanistic approaches for CO_2 storage integrity. *Energies* **2026**, *19*, 1154. [CrossRef]
17. Vo Thanh, H.; Sugai, Y.; Sasaki, K. Application of artificial neural network for predicting the performance of CO_2 enhanced oil recovery and storage in residual oil zones. *Sci. Rep.* **2020**, *10*, 18204. [CrossRef] [PubMed]
18. Dai, Z.; Middleton, R.; Viswanathan, H.; Fessenden-Rahn, J.; Bauman, J.; Pawar, R.; Lee, S.-Y.; McPherson, B. An integrated framework for optimizing CO_2 sequestration and enhanced oil recovery. *Environ. Sci. Technol. Lett.* **2014**, *1*, 49–54. [CrossRef]
19. Chen, B.; Harp, D.R.; Lin, Y.; Keating, E.H.; Pawar, R.J. Geologic CO_2 sequestration monitoring design: A machine learning and uncertainty quantification based approach. *Appl. Energy* **2018**, *225*, 332–345. [CrossRef]
20. Haghighat, S.A.; Mohaghegh, S.D.; Gholami, V.; Shahkarami, A.; Moreno, D.A. Using big data and smart field technology for detecting leakage in a CO_2 storage project. In Proceedings of the SPE Annual Technical Conference and Exhibition, New Orleans, LA, USA, 30 September–2 October 2013. [CrossRef]
21. Ashraf, U.; Zhu, P.; Yasin, Q.; Anees, A.; Imraz, M.; Mangi, H.N.; Shakeel, S. Classification of reservoir facies using well log and 3D seismic attributes for prospect evaluation and field development: A case study of Sawan gas field. *J. Pet. Sci. Eng.* **2019**, *175*, 338–351. [CrossRef]
22. Wang, J.; Song, Z.; Chen, L.; Xu, T.; Deng, L.; Qi, Z. Prediction of CO_2 solubility in deep eutectic solvents using random forest model based on COSMO-RS-derived descriptors. *Green Chem. Eng.* **2021**, *2*, 431–440. [CrossRef]
23. Venkatraman, V.; Alsberg, B.K. Predicting CO_2 capture of ionic liquids using machine learning. *J. CO_2 Util.* **2017**, *21*, 162–168. [CrossRef]
24. Baghban, A.; Sasanipour, J.; Zhang, Z. A new chemical structure-based model to estimate solid compound solubility in supercritical CO_2. *J. CO_2 Util.* **2018**, *26*, 262–270. [CrossRef]
25. Dashti, A.; Bahrololoomi, A.; Amirkhani, F.; Mohammadi, A.H. Estimation of CO_2 adsorption in high capacity metal organic frameworks: Applications to greenhouse gas control. *J. CO_2 Util.* **2020**, *41*, 101256. [CrossRef]
26. Mohammadi, M.-R.; Hadavimoghaddam, F.; Pourmahdi, M.; Atashrouz, S.; Munir, M.T.; Hemmati-Sarapardeh, A.; Mosavi, A.H.; Mohaddespour, A. Modeling hydrogen solubility in hydrocarbons using extreme gradient boosting and equations of state. *Sci. Rep.* **2021**, *11*, 17911. [CrossRef] [PubMed]
27. Wen, Y.; Wu, R.; Zhou, Z.; Zhang, S.; Yang, S.; Wallington, T.J.; Shen, W.; Tan, Q.; Deng, Y.; Wu, Y. A data-driven method of traffic emissions mapping with land use random forest models. *Appl. Energy* **2022**, *305*, 117916. [CrossRef]
28. Fang, Y.; Lu, X.; Li, H. A random forest-based model for the prediction of construction-stage carbon emissions at the early design stage. *J. Clean. Prod.* **2021**, *328*, 129657. [CrossRef]
29. Ahmad, M.W.; Reynolds, J.; Rezgui, Y. Predictive modelling for solar thermal energy systems: A comparison of support vector regression, random forest, extra trees and regression trees. *J. Clean. Prod.* **2018**, *203*, 810–821. [CrossRef]
30. Saghafi, H.; Ghiasi, M.M.; Mohammadi, A.H. Analyzing the experimental data of CO_2 equilibrium absorption in the aqueous solution of DEA + MDEA with Random Forest and Leverage method. *Int. J. Greenh. Gas Control* **2017**, *63*, 329–337. [CrossRef]
31. Zhu, X.; Tsang, D.C.W.; Wang, L.; Su, Z.; Hou, D.; Li, L.; Shang, J. Machine learning exploration of the critical factors for CO_2 adsorption capacity on porous carbon materials at different pressures. *J. Clean. Prod.* **2020**, *273*, 122915. [CrossRef]

32. Nait Amar, M.; Zeraibi, N. Application of hybrid support vector regression artificial bee colony for prediction of MMP in CO_2-EOR process. *Petroleum* **2020**, *6*, 415–422. [CrossRef]
33. Gupta, S.; Li, L. The potential of machine learning for enhancing CO_2 sequestration, storage, transportation, and utilization-based processes: A brief perspective. *JOM* **2022**, *74*, 414–428. [CrossRef]
34. Rehman, A.N.; Lal, B. Machine learning in CO_2 sequestration. In *Machine Learning and Flow Assurance in Oil and Gas Production*; Lal, B., Bavoh, C.B., Sahith Sayani, J.K., Eds.; Springer: Berlin/Heidelberg, Germany, 2023. [CrossRef]
35. Alsubaih, A.; Sepehrnoori, K.; Delshad, M. Development and optimization of self-healing cement for CO_2 injection and storage wells: Enhancing long-term wellbore integrity in extreme subsurface conditions. *Appl. Sci.* **2025**, *15*, 5428. [CrossRef]
36. Yan, B.; Chen, B.; Harp, D.R.; Pawar, R.J. A robust deep learning workflow to predict multiphase flow behavior during geological CO_2 sequestration Injection and Post-Injection Periods. *arXiv* **2022**, arXiv:2107.07274.
37. Ford, E.P.; Moeinikia, F.; Lohne, H.P.; Arild, O.; Majoumerd, M.M.; Fjelde, K.K. Leakage Calculator for Plugged and Abandoned Wells. In Proceedings of the Society of Petroleum Engineers-SPE Bergen One Day Seminar, Bergen, Norway, 5 April 2017. [CrossRef]
38. Shi, X.; Yang, Y.; Liao, Y.; Wang, D.; Han, S.; Gao, Q. Unconfined Compressive Strength Estimation in the Shale Gas Reservoir Using Data Driven Technique. In *Proceedings of the 57th U.S. Rock Mechanics/Geomechanics Symposium*; ARMA-2023-0255; ARMA: Alexandria, VA, USA, 2023. [CrossRef]
39. Sanei, M.; Ramezanzadeh, A.; Asgari, A. Building 1D and 3D static reservoir geomechanical properties models in the oil field. *J. Pet. Explor. Prod. Technol.* **2023**, *13*, 329–351.
40. Malkowski, P.; Ostrowski, L. The Methodology for the Young Modulus Derivation for Rocks and Its Value. In *Proceedings of the ISRM European Rock Mechanics Symposium-EUROCK 2017*; ISRM-EUROCK-2017-018; ISRM: Lisbon, Portugal, 2017.
41. Sadeghpour, S.; Gao, Y.; Motra, H.B.; Hajdiijej, F. Comparison of geomechanical upscaling methods for prediction of elastic modulus of heterogeneous media. *Geoenergy Sci. Eng.* **2024**, *239*, 212915. [CrossRef]
42. Eaton, B.A. Fracture Gradient Prediction and Its Application in Oilfield Operations. *J. Pet. Technol.* **1969**, *21*, 1353–1360. [CrossRef]
43. Greaves, G.N.; Greer, A.L.; Lakes, R.S.; Rouxel, T. Poisson's ratio and modern materials. *Nat. Mater.* **2011**, *10*, 823–837. [PubMed]
44. Abbas, A.K.; Alsaba, M.T.; Flori, R. Geomechanical Modeling and Wellbore Stability Analysis Approach to Plan Deep Horizontal Wells Across Problematic Shale Formation. In *Proceedings of the Unconventional Resources Technology Conference*; SPE: Richardson, TX, USA, 2018.
45. Gowida, A.; Elkatatny, S.; Gamal, H. Unconfined compressive strength (UCS) prediction in real-time while drilling using artificial intelligence tools. *Neural Comput. Appl.* **2021**, *33*, 8043–8054. [CrossRef]
46. Siddig, O.; Gamal, H.; Elkatatny, S.; Abdulraheem, A. Real-time prediction of Poisson's ratio from drilling parameters using machine learning tools. *Sci. Rep.* **2021**, *11*, 12611. [CrossRef] [PubMed]
47. Na, S.R.; Shadizadeh, S.R.; Riahi, M.A.; Mirzakhanian, M. Estimation of reservoir porosity and water saturation based on seismic attributes using support vector regression approach. *J. Appl. Geophys.* **2014**, *107*, 93–101. [CrossRef]
48. Song, J.; Zhang, D. Comprehensive review of caprock-sealing mechanisms for geologic carbon sequestration. *Environ. Sci. Technol.* **2013**, *47*, 9–22. [CrossRef] [PubMed]
49. Li, Y.; Sun, Y. Modeling and predicting city-level CO_2 emissions using open access data and machine learning. *Environ. Sci. Pollut. Res.* **2021**, *28*, 19260–19271. [CrossRef] [PubMed]
50. Abdi, J.; Hadavimoghaddam, F.; Hadipoor, M.; Hemmati-Sarapardeh, A. Modeling of CO_2 adsorption capacity by porous metal organic frameworks using advanced decision tree-based models. *Sci. Rep.* **2021**, *11*, 24468. [CrossRef] [PubMed]
51. Ma, J.; Ding, Y.; Cheng, J.C.P.; Jiang, F.; Tan, Y.; Gan, V.J.L.; Wan, Z. Identification of high impact factors of air quality on a national scale using big data and machine learning techniques. *J. Clean. Prod.* **2020**, *244*, 118955. [CrossRef]
52. Fan, J.; Wu, L.; Zhang, F.; Cai, H.; Zeng, W.; Wang, X. Empirical and machine learning models for predicting daily global solar radiation from sunshine duration: A review and case study in China. *Renew. Sustain. Energy Rev.* **2019**, *100*, 186–212. [CrossRef]
53. Ji, X.; Zhu, C. CO_2 storage in deep saline aquifers. In *Novel Materials for Carbon Dioxide Mitigation Technology*; Elsevier: Amsterdam, The Netherlands, 2015; pp. 299–332. [CrossRef]
54. Chow, J.C.; Watson, J.G.; Herzog, A.; Benson, S.M.; Hidy, G.M.; Gunter, W.D.; Penkala, S.J.; White, C.M. Separation and capture of CO_2 from large stationary sources and sequestration in geological formations. *J. Air Waste Manag. Assoc.* **2003**, *53*, 1172–1182. [CrossRef] [PubMed]
55. Safaei-Farouji, M.; Vo Thanh, H.; Dai, Z.; Mehbodniya, A.; Rahimi, M.; Ashraf, U.; Radwan, A.E. Exploring the power of machine learning to predict carbon dioxide trapping efficiency in saline aquifers for carbon geological storage project. *J. Clean. Prod.* **2022**, *372*, 133778. [CrossRef]
56. Abdulkhaleq, H.B.; Ibraheem, I.K.; Al-Mudhafar, W.J.; Mohammed, Z.T.; Abd, M.S. Harnessing the power of machine learning for the optimization of CO_2 sequestration in saline aquifers: Applied on the Tensleep formation at Teapot Dome in Wyoming. *Geoenergy Sci. Eng.* **2025**, *245*, 213522.

57. Abdulwahab, S.M.; Al-Mudhafar, W.J.; Sepehrnoori, K.; Al Aulaqi, T. Proxy-based multi-objective optimization of CO_2-EOR and geological storage using NN-RBF and DWS-assisted pressure management. In *SPE Conference at Oman Petroleum & Energy Show, Muscat, Oman*; SPE-232602-MS; SPE: Richardson, TX, USA, 2026. [CrossRef]
58. Al-Mudhafar, W.; Al-Abdulwahid, R.Y. Optimizing CO_2 sequestration in fully water-saturated reservoirs: Machine learning-based enhanced trapping efficiency in South Rumaila Field. In *The 87th EAGE Annual Conference & Exhibition*; EAGE: Houten, The Netherlands, 2026; Volume 2026, pp. 1–5. [CrossRef]
59. Chen, J.; Lu, L.; Sidahmed, M.; Bai, T.; Folmar, I.; Seth, P.; Sarfare, M.; Mikulencak, D.; Akil, I. Machine learning in automating carbon sequestration site assessment. In *NeurIPS Workshop on Tackling Climate Change with ML*; Climate Change AI: Montreal, QC, Canada, 2021. Available online: https://www.climatechange.ai/papers/neurips2021/62 (accessed on 14 May 2026).
60. Wang, Z.; Chen, Y.; Chen, G.; Zhang, D. Optimization of geological carbon storage operations with multimodal latent dynamic model and deep reinforcement learning. *arXiv* **2024**, arXiv:2406.04575.
61. Tirapu Azpiroz, J.; Giro, R.; Ferreira, R.N.B.; da Silva, M.N.P.; Rodriguez, M.F.B.; Lopez, A.E.C.; Vasquez, D.A.L.; Ferreira, M.E.; Del Grande, M.; Da Silva, A.F.; et al. Optimizing carbon dioxide trapping for geological storage. *arXiv* **2023**, arXiv:2312.13512.
62. Kadeethum, T.; Verzi, S.J.; Yoon, H. Efficient machine-learning surrogates for large-scale geological carbon and energy storage. *arXiv* **2023**, arXiv:2310.07461.
63. Graham, G.H.; Chen, Y. Bayesian inversion of generative models for geologic storage of carbon dioxide. *arXiv* **2020**, arXiv:2001.04829.
64. Wu, J.; Zhou, M.; Li, Z. Machine learning-based geological modeling for CO_2 storage site selection. *IEEE Trans. Geosci. Remote Sens.* **2020**, *58*, 8984–8995. [CrossRef]
65. Damico, J.R.; Cole, K.S.; Bentley, L.R. Carbon storage assessment in the Illinois Basin using machine learning techniques. *IEEE Access* **2021**, *9*, 102345–102359. [CrossRef]
66. Zhong, C.; Huang, Z.; Tang, M.; Zhang, Y. Real-time anomaly detection for carbon storage monitoring using ConvLSTM networks. *Comput. Geosci.* **2019**, *132*, 104323. [CrossRef]
67. Zhang, Y.; Zhang, J.; Li, S.; Wang, H. Hybrid CNN-BiLSTM model for CO_2 storage anomaly detection using bottomhole pressure data. *J. Pet. Sci. Eng.* **2022**, *208*, 109230. [CrossRef]
68. Steer, H.S. The Geomechanical Model for Carbon Dioxide Storage in East Baghdad Oil Field. Master's Thesis, University of Baghdad, Baghdad, Iraq, 2022.
69. Kadhim, M.M.J. Carbon Dioxide Storage in Subsurface Formations for Enhanced Hydrocarbon Recovery: Siba Oil Field—Nahr Umar Formation. Master's Thesis, University of Baghdad, Baghdad, Iraq, 2024.
70. Nicot, J.P.; Oldenburg, C.M.; Bryant, S.L.; Hovorka, S.D. Pressure perturbations from geologic carbon sequestration: Area-of-review boundaries and borehole leakage driving forces. *Energy Procedia* **2009**, *1*, 47–54. [CrossRef]
71. Gupta, P.K.; Sharma, S.; Jain, L.K. Real-time CO_2 leakage monitoring using artificial intelligence in carbon capture projects. *IEEE Trans. Ind. Inform.* **2021**, *17*, 4021–4032. [CrossRef]
72. Gorecki, C.D.; Hamling, J.A.; Ensrud, J.; Steadman, E.N.; Harju, J.A. Integrating CO_2 EOR and CO_2 storage in the Bell Creek oil field. In *Carbon Management Technology Conference*; SPE: Richardson, TX, USA, 2012. [CrossRef]
73. Ma, J.-F.; Li, L.; Wang, H.-F.; Tan, M.-Y.; Cui, S.-L.; Zhang, Y.-Y.; Qu, Z.-P.; Jia, L.-Y.; Zhang, S.-H. Geophysical monitoring technology for CO_2 sequestration. *Appl. Geophys.* **2016**, *13*, 288–306. [CrossRef]
74. Myrttinen, A.; Becker, V.; Nowak, M.; Zimmer, M.; Pilz, P.; Barth, J.A.C. Analyses of pre-injection reservoir data for stable carbon isotope trend predictions in CO_2 monitoring. *Environ. Earth Sci.* **2012**, *67*, 473–479. [CrossRef]
75. Ghoreishi-Madiseh, S.A.; Sadrzadeh, M. Optimization of CO_2 injection and brine production well placement using artificial neural networks. *Int. J. Greenh. Gas Control* **2013**, *15*, 112–122. [CrossRef]
76. He, J.; Lin, M.; Zhang, Y. Deep learning-based direct forecasting of CO_2 plume migration. *Adv. Geo-Energy Res.* **2022**, *6*, 59–71. [CrossRef]
77. Cihan, A.; Zhou, Q.; Birkholzer, J.T. Analytical solutions for pressure perturbation and fluid leakage through aquitards and wells in multilayered-aquifer systems. *Water Resour. Res.* **2011**, *47*, 10504. [CrossRef]
78. Al-Khdheewai, E.A.; Vialle, S.; Barifcani, A.; Sarmadivaleh, M.; Iglauer, S. Enhancement of CO_2 trapping efficiency in heterogeneous reservoirs by water-alternating gas injection. *Greenh. Gases Sci. Technol.* **2018**, *8*, 920–931.
79. Almansor, A.; Al-Iedani, A.; Al-Mudhafar, W. Evaluation of Downhole Water Sink technology for efficient CO_2 sequestration in the South Rumaila oil field. In *The 86th EAGE Annual Conference & Exhibition*; EAGE: Houten, The Netherlands, 2026; Volume 2025, pp. 1–5. [CrossRef]
80. Li, Y.; Sun, Y.; Lin, J. Learning CO_2 plume migration in faulted reservoirs with Graph Neural Networks. *J. Pet. Sci. Eng.* **2023**, *215*, 110631. [CrossRef]
81. Chen, J.; Gildin, E.; Kompantsev, G. Optimization of Pressure Management Strategies for Geological CO_2 Sequestration Using Surrogate Model-based Reinforcement Learning. *arXiv* **2023**, arXiv:2403.07360.

82. Raissi, M.; Perdikaris, P.; Karniadakis, G.E. Physics-Informed Neural Networks: A Deep Learning Framework for Solving Forward and Inverse Problems Involving Nonlinear Partial Differential Equations. *J. Comput. Phys.* **2019**, *378*, 686–707. [CrossRef]
83. Fuks, O.; Tchelepi, H.A. Limitations of physics informed machine learning for nonlinear two-phase transport in porous media. *J. Mach. Learn. Model. Comput.* **2020**, *1*, 19–37. [CrossRef]
84. Harp, D.R.; O'Malley, D.; Yan, B.; Pawar, R. On the feasibility of using physics-informed machine learning for underground reservoir pressure management. *Expert Syst. Appl.* **2021**, *178*, 115006. [CrossRef]
85. Wang, Y.; Vuik, C.; Hajibeygi, H. Analysis of hydrodynamic trapping interactions during full-cycle injection and migration of CO_2 in deep saline aquifers. *Adv. Water Resour.* **2022**, *159*, 104073. [CrossRef]
86. Darvishpour, A.; Cheraghi, S.M.; David, A.; Ghorbani, H. Wellbore stability analysis to determine the safe mud weight window for sandstone layers. *Pet. Explor. Dev.* **2019**, *46*, 1031–1038. [CrossRef]
87. Altmann, J.B.; Müller, B.I.R.; Müller, T.M.; Heidbach, O.; Tingay, M.R.P.; Weißhardt, A. Pore pressure stress coupling in 3D and consequences for reservoir stress states and fault reactivation. *Geothermics* **2014**, *52*, 195–205. [CrossRef]
88. Khan, S.; Khulief, Y.A.; Al-Shuhail, A.A. Effects of reservoir size and boundary conditions on pore-pressure buildup and fault reactivation during CO_2 injection. *Environ. Earth Sci.* **2020**, *79*, 294. [CrossRef]
89. Ye-Jun, J.; Ling-Dong, M.; Ding-You, L.; Xiao-Fei, F.; Jiang-Bo, H.; Si-Jia, C.; Jian-Da, L. Risk assessment of fault reactivation considering the heterogeneity of friction strength. *Pet. Sci.* **2023**, *20*, 2695–2708. [CrossRef]
90. Zhou, Y. A pressure-monitoring method to warn CO_2 leakage in geological storage reservoirs. *Environ. Earth Sci.* **2021**. [CrossRef]
91. Dempsey, D.; Kelkar, S.; Pawar, R. A strategy for mitigating reservoir pressurization, induced seismicity and brine migration in geologic CO_2 storage. *Int. J. Greenh. Gas Control* **2014**, *28*, 96–113.
92. Alshalabi, A.; Al Saadi, H.; Maire, F.; Thomas, T.; Gueye, T.; Al Amiri, F. A Major Shift in Reservoir Management Strategies and Best Practices in a Mature Reservoir. In *Proceedings of the Abu Dhabi International Petroleum Exhibition & Conference*; SPE-203313-MS; SPE: Richardson, TX, USA, 2020. [CrossRef]
93. Sifuentes, W.; Mandal, D.; Kumaran, P.N.; Ibrahim, R.; Chabernaud, T.; Ceccarelli, T.; Moreno, J.C.; Sepulveda, W. Addressing Key Risks Through Sound Reservoir Management. In *Proceedings of the SPE Asia Pacific Oil and Gas Conference and Exhibition*; SPE-191995-MS; SPE: Richardson, TX, USA, 2018. [CrossRef]
94. Abdulwahab, S.M.; Al-Mudhafar, W.J.; Abdul-Majeed, G.H.; Sepehrnoori, K. Feasibility of Downhole Water Sink-assisted CO_2 sequestration: A scalable data-driven framework. In *SPE/AAPG/SEG Unconventional Resources Technology Conference, Houston, Texas, USA*; SPE: Richardson, TX, USA, 2026.
95. Sambo, C.; Iferobia, C.C.; Babasafari, A.A.; Rezaei, S.; Akanni, O.A. The role of time-lapse (4D) seismic technology as reservoir monitoring and surveillance tool: A comprehensive review. *J. Nat. Gas Sci. Eng.* **2020**, *80*, 103312. [CrossRef]
96. Verdon, J.P.; Kendall, J.M.; White, D.J.; Angus, D.A.; Fisher, Q.J.; Urbancic, T. Passive seismic monitoring of carbon dioxide storage at Weyburn. *Lead. Edge* **2010**, *29*, 200–206. [CrossRef]
97. Paulsson, B.N.P. Crosswell and single-well seismic monitoring of CO_2 sequestration. *Lead. Edge* **2006**, *25*, 1534–1542. [CrossRef]
98. Xue, Z.; Mito, S.; Ohsumi, T. Time-lapse well logging for monitoring CO_2 behavior at the Nagaoka pilot site. *Energy* **2006**, *31*, 2972–2980. [CrossRef]
99. Jackson, S.J.; Gunning, J.; Ennis-King, J.; Dance, T.; Pevzner, R.; Dumesny, P.; Barraclough, P.; Jenkins, C. Tracking a subsurface CO_2 plume with time-lapse pressure tomography in the Otway Stage 3 field project. *Int. J. Greenh. Gas Control* **2024**, *133*, 104099. [CrossRef]
100. Ajo-Franklin, J.B.; Daley, T.M.; Peterson, J.E. High-resolution 3D surface seismic imaging for monitoring CO_2 injection in a shallow unconsolidated sand reservoir. *Geophysics* **2013**, *78*, Q51–Q63. [CrossRef]
101. Ajayi, T.; Gomes, J.S.; Bera, A. A review of CO_2 storage in geological formations emphasizing modeling, monitoring and capacity estimation approaches. *Pet. Sci.* **2019**, *16*, 1028–1063. [CrossRef]
102. Sun, Y.; Xue, Z.; Park, H.; Hashimoto, T.; Zhang, Y. Optical sensing of CO_2 geological storage using distributed fiber-optic sensor: From laboratory to field-scale demonstrations. *Energy Fuels* **2021**, *35*, 659–669. [CrossRef]
103. Watson, T.B.; Sullivan, T. Feasibility of a Perfluorocarbon tracer-based network to support monitoring, verification, and accounting of sequestered CO_2. *Environ. Sci. Technol.* **2012**, *46*, 1692–1699. [CrossRef] [PubMed]
104. Verkerke, J.L.; Williams, D.J.; Thoma, E. Remote sensing of CO_2 leakage from geologic sequestration projects. *Int. J. Appl. Earth Obs. Geoinf.* **2014**, *31*, 67–77. [CrossRef]
105. Tiab, D.; Donaldson, E.C. *Petrophysics*, 4th ed.; Elsevier: Boston, MA, USA, 2016. [CrossRef]
106. Liu, M.; Grana, D. Petrophysical characterization of deep saline aquifers for CO_2 storage using ensemble smoother and deep convolutional autoencoder. *Adv. Water Resour.* **2020**, *142*, 103634. [CrossRef]
107. Jiang, Z.; Liu, N.; Zhang, Y. Pore-scale modeling and visualization of CO_2 displacement and trapping in heterogeneous sandstone. *Fuel* **2017**, *207*, 80–89. [CrossRef]
108. Soong, Y.; Goodman, A.; McCarthy-Jones, J.R. Use of micro-CT imaging and modeling to evaluate CO_2 trapping mechanisms in sandstone. *Int. J. Greenh. Gas Control* **2014**, *27*, 13–23. [CrossRef]

109. De, A.; Shukla, K.; Agarwal, R.K. Application of microfluidic and pore-scale imaging in understanding CO_2 displacement efficiency. *Adv. Water Resour.* **2021**, *149*, 103852. [CrossRef]
110. Busch, A.; Hangx, S.; Vialle, S.; Rizzo, R.E.; Kampman, N. Mechanical weakening of a mudrock seal by reaction with CO_2-charged fluids. *Geology* **2023**, *51*, 616–620. [CrossRef]
111. Petrovic, S.; Osei, J.; Rostami, B. Gravimetric and manometric adsorption of CO_2 in coal and shale: A critical review. *J. Nat. Gas Sci. Eng.* **2022**, *100*, 104519. [CrossRef]
112. Abdulkareem, O.A.; Bader, M.R.; Alharthy, N.; Kamal, M.S. Experimental investigation of CO_2 adsorption in shale for enhanced gas recovery and carbon sequestration. *J. Nat. Gas Sci. Eng.* **2020**, *81*, 103437. [CrossRef]
113. Udebhulu, A.E.; Wang, X.; Liu, S.; Agbasi, C.E. Machine learning application for leakage detection and risk management in geological carbon sequestration: A review. *Environ. Sci. Pollut. Res.* **2024**, *31*, 1–20. [CrossRef]
114. Govindan, R.; Agarwal, A.; Al-Anazi, A. A remote sensing and geostatistical approach for leakage detection in CO_2 storage sites. *Int. J. Greenh. Gas Control* **2011**, *5*, 1449–1459. [CrossRef]
115. Bakhshian, S.; Romanak, K.D. DeepSense: A deep learning-based framework for detecting CO_2 leakage in geological storage. *Environ. Model. Softw.* **2021**, *137*, 104973. [CrossRef]
116. Sinha, A.; Rao, V.; Verma, N. Artificial neural networks for identifying leakage anomalies in carbon capture and storage projects. *Energy Rep.* **2020**, *6*, 215–223. [CrossRef]
117. Xin, Y.; Liu, B.; Zhou, J. Outlier detection using subspace local outlier factor for CO_2 leakage detection. *Expert Syst. Appl.* **2015**, *42*, 8449–8461. [CrossRef]
118. Min, K.; Kim, J.; Lee, H. Detection of sinusoidal leakage patterns in CCS sites using frequency domain analysis. *J. Clean. Prod.* **2018**, *198*, 1230–1240. [CrossRef]
119. Holloway, S.; Pearce, J.M.; Hards, V.L.; Ohsumi, T.; Gale, J. Natural emissions of CO_2 from the geosphere and their bearing on the geological storage of carbon dioxide. *Energy* **2006**, *32*, 1194–1201. [CrossRef]
120. Williams, D.J. *Toxicological Profile for Carbon Dioxide*; Agency for Toxic Substances and Disease Registry, U.S. Department of Health and Human Services: Atlanta, GA, USA, 1995.
121. Beaubien, S.E.; Ciotoli, G.; Lombardi, S. Carbon dioxide seepage through faults and fractures in the Apennines, Italy: Implications for long-term leakage from geologic storage sites. *Int. J. Greenh. Gas Control* **2008**, *2*, 356–372. [CrossRef]
122. Bowden, J. Safe storage of CO_2 underground: A review of acceptable leakage rates. *Geol. Soc. Spec. Publ.* **2005**, *233*, 1–14. [CrossRef]
123. Lele, S.P.; Tyrrell, T.E.; deMartin, B.J. Effect of Faulting Regime, Poisson's Ratio, and Non-Uniform Reservoir Deformation on Fault Reactivation Due to Injection and Production. In *Proceedings of the 54th U.S. Rock Mechanics/Geomechanics Symposium*; ARMA-2020-1595; ARMA: Alexandria, VA, USA, 2020.
124. Guglielmi, Y.; Nussbaum, C.; Cappa, F.; De Barros, L.; Rutqvist, J.; Birkholzer, J. Field-scale fault reactivation experiments by fluid injection highlight aseismic leakage in caprock analogs: Implications for CO_2 sequestration. *Int. J. Greenh. Gas Control* **2021**, *111*, 103471. [CrossRef]
125. Alsubaih, A.; Sepehrnoori, K.; Delshad, M. Environmental impacts of orphaned and abandoned wells: Methane emissions, and implications for carbon storage. *Appl. Sci.* **2024**, *14*, 11518. [CrossRef]
126. Nordbotten, J.M.; Celia, M.A.; Bachu, S. Analytical solutions for leakage rates through abandoned wells. *Water Resour. Res.* **2004**, *40*, W04204. [CrossRef]
127. Qiao, T.; Hoteit, H.; Fahs, M. Semi-analytical solution to assess CO_2 leakage in the subsurface through abandoned wells. *Energies* **2021**, *14*, 2452. [CrossRef]
128. Aker, E.; Skurtveit, E.; Oye, V. InSAR detection of surface uplift related to CO_2 injection at In Salah, Algeria. *Int. J. Greenh. Gas Control* **2011**, *5*, 939–951. [CrossRef]
129. Klinginger, A. CO_2 migration in deep saline aquifers: The influence of permeability and geologic structure. *Transp. Porous Media* **2006**, *65*, 517–536. [CrossRef]
130. Andreas, L. Thermal effects on CO_2 mobility and storage performance in saline aquifers. *Geothermics* **2008**, *37*, 473–483. [CrossRef]
131. Onuma, T. Assessment of potential leakage during CO_2 geological storage using integrated modeling. *Energy Procedia* **2009**, *1*, 2831–2838. [CrossRef]
132. Juhlin, C.; Giese, R.; Zinck-Jørgensen, K.; Cosma, C.; Kazemeini, H.; Juhojuntti, N.; Lüth, S.; Norden, B.; Förster, A. 3D baseline seismics at the CO_2SINK site, Ketzin, Germany. *Geophysics* **2007**, *72*, B121–B132. [CrossRef]
133. Hilke, H.; Norden, B.; Förster, A.; Juhlin, C. 3D geological modeling for CO_2 storage at the Ketzin site. *Int. J. Greenh. Gas Control* **2010**, *4*, 973–984. [CrossRef]
134. Bachu, S.; Bonijoly, D.; Bradshaw, J.; Burruss, R.; Holloway, S.; Christensen, N.P.; Mathiassen, O.M. CO_2 storage capacity estimation: Methodology and gaps. *Int. J. Greenh. Gas Control* **2007**, *1*, 430–443. [CrossRef]
135. Duan, Z.; Sun, R. An improved model calculating CO_2 solubility in pure water and aqueous NaCl solutions. *Chem. Geol.* **2003**, *193*, 257–271. [CrossRef]

136. Averill, B.A.; Eldredge, P. *Principles of General Chemistry*; Cengage Learning: Boston, MA, USA, 2012.
137. Gross, P.M. The "salting-out" of non-electrolytes from aqueous solutions. *Chem. Rev.* **1933**, *13*, 91–111. [CrossRef]
138. Pan, L. Modified CO_2 solubility models for accurate predictions in complex brines. *J. Chem. Thermodyn.* **2018**, *125*, 123–135. [CrossRef]
139. Duan, Z.; Sun, R.; Zhu, C.; Chou, I.M. An improved model for the calculation of CO_2 solubilities in aqueous solutions containing Na^+, K^+, Ca^{2+}, Mg^{2+}, Cl^-, and SO_4^{2-}. *Mar. Chem.* **2006**, *98*, 131–139. [CrossRef]
140. Sayegh, S.G. CO_2-brine interactions: pH changes and mineral precipitation in carbonate formations. *J. Pet. Sci. Eng.* **1990**, *4*, 201–214. [CrossRef]
141. Liu, D.; Zhang, Z.; Yang, S.; Yu, Q.; Agarwal, R.K.; Li, Y. Role of permeability evolution induced by CO_2 injection on CO_2 storage and CH_4 production in a low permeability reservoir. *Chem. Geol.* **2025**, *694*, 123014. [CrossRef]
142. Yang, Y.; Ju, B.; Lü, G.; Huang, Y. Machine learning methods for predicting CO_2 solubility in hydrocarbons. *Pet. Sci.* **2024**, *21*, 3340–3349. [CrossRef]
143. Al-qaness, M.A.A.; Ewess, A.A.; Vo Thanh, H.; AlRassas, A.M.; Abd Elaziz, M. An optimized neuro-fuzzy system using advance nature-inspired Aquila and Salp swarm algorithms for smart predictive residual and solubility carbon trapping efficiency in underground storage formations. *J. Energy Storage* **2022**, *55*, 106150.
144. Wang, N.; Durlofsky, L.J. Deep learning framework for history matching CO_2 storage with 4D seismic and monitoring well data. *Geoenergy Sci. Eng.* **2025**, *248*, 213736.
145. Zhang, Y.; Song, J.; Liu, H. Machine learning-based site selection for carbon sequestration in deep geological formations. *Greenh. Gases Sci. Technol.* **2021**, *11*, 888–900. [CrossRef]
146. Pradoo, P.; Jacobs, B.; Hill, K.; Wilkes, S.; Ruffini, J.; Srisang, W.; Feng, Y.; Daverne, D.; Nelson, C. Improving the operating availability of the Boundary Dam Unit 3 carbon capture facility. In Proceedings of the 16th Greenhouse Gas Control Technologies Conference (GHGT-16), Lyon, France, 23–27 October 2022.
147. Al-Khudhairy, D.H.; Løseth, H. AI-assisted seismic data interpretation for CO_2 storage site characterization: A Sleipner case study. *First Break* **2021**, *39*, 67–72. [CrossRef]
148. Ringrose, P.S.; Meckel, T.A. Maturing global CO_2 storage resources on offshore continental margins to achieve 2DS emissions reductions. *Sci. Rep.* **2019**, *9*, 17944. [CrossRef] [PubMed]
149. Baklid, A.; Korbøl, R.; Owren, G. Sleipner Vest CO_2 disposal, CO_2 injection into a shallow underground aquifer. In Proceedings of the SPE Annual Technical Conference and Exhibition, Denver, CO, USA, 6–9 October 1996.
150. Chadwick, A.; Arts, R.; Eiken, O.; Zweigel, P.; van der Meer, L.; Zinszner, B. 4D seismic imaging of a CO_2 plume at the Sleipner Field, central North Sea. *Pet. Geosci.* **2004**, *10*, 133–140. [CrossRef]
151. Global CCS Institute. *The Global Status of CCS 2021*; Global CCS Institute: Melbourne, Australia, 2021.
152. Timperley, J. *Gorgon Carbon Capture and Storage Project: The Failure of the World's Largest CCS Facility*; Medium: San Francisco, CA, USA, 2021. Available online: https://timinclimate.medium.com/gorgon-carbon-capture-and-storage-project-the-failure-of-the-worlds-largest-ccs-facility-d517de0ee176 (accessed on 14 May 2026).
153. Michael, K.; Golab, A.; Shulakova, V.; Ennis-King, J.; Allinson, G.; Sharma, S.; Aiken, T. Geological storage of CO_2 in saline aquifers—A review of the experience from existing storage operations. *Int. J. Greenh. Gas Control* **2010**, *4*, 659–667. [CrossRef]
154. Chevron. *Gorgon Carbon Capture and Storage Fact Sheet*; Chevron: Perth, Australia, 2021.
155. Arts, R.; Eiken, O.; Chadwick, A.; Zweigel, P.; van der Meer, L.; Zinszner, B. Monitoring of CO_2 injected at Sleipner using time-lapse seismic data. *Energy* **2004**, *29*, 1383–1392. [CrossRef]
156. Nooner, S.L.; Vasco, D.W. Monitoring storage of CO_2 using combined seismic and gravity data at Sleipner. *Geophysics* **2014**, *79*, B107–B117. [CrossRef]
157. Zweigel, P.; Arts, R.; Lothe, A.E.; Lindeberg, E. Reservoir geology of the Utsira Formation at the first industrial-scale underground CO_2 storage site (Sleipner area, North Sea). In *Geological Storage of Carbon Dioxide for Emissions Reduction*; Baines, S., Gale, J., Worden, R., Eds.; Geological Society: London, UK, 2004; pp. 165–180.
158. Shell Canada. *Annual Report 2022*; Shell Canada: Calgary, AB, Canada, 2022; pp. 46–50.
159. Government of Alberta. *Quest Carbon Capture and Storage Project: Environmental Impact Assessment*; Government of Alberta: Edmonton, AB, Canada, 2020; pp. 12–15.